Jackson School of Geosciences 15th Annual Symposium

Friday, February 6th, San Jacinto Multipurpose Room (SJH Building)

Google Map Link Location: https://maps.app.goo.gl/J1fwEzPV3TMGivH18

Symposium Website Link: https://www.jsg.utexas.edu/research_symposium/

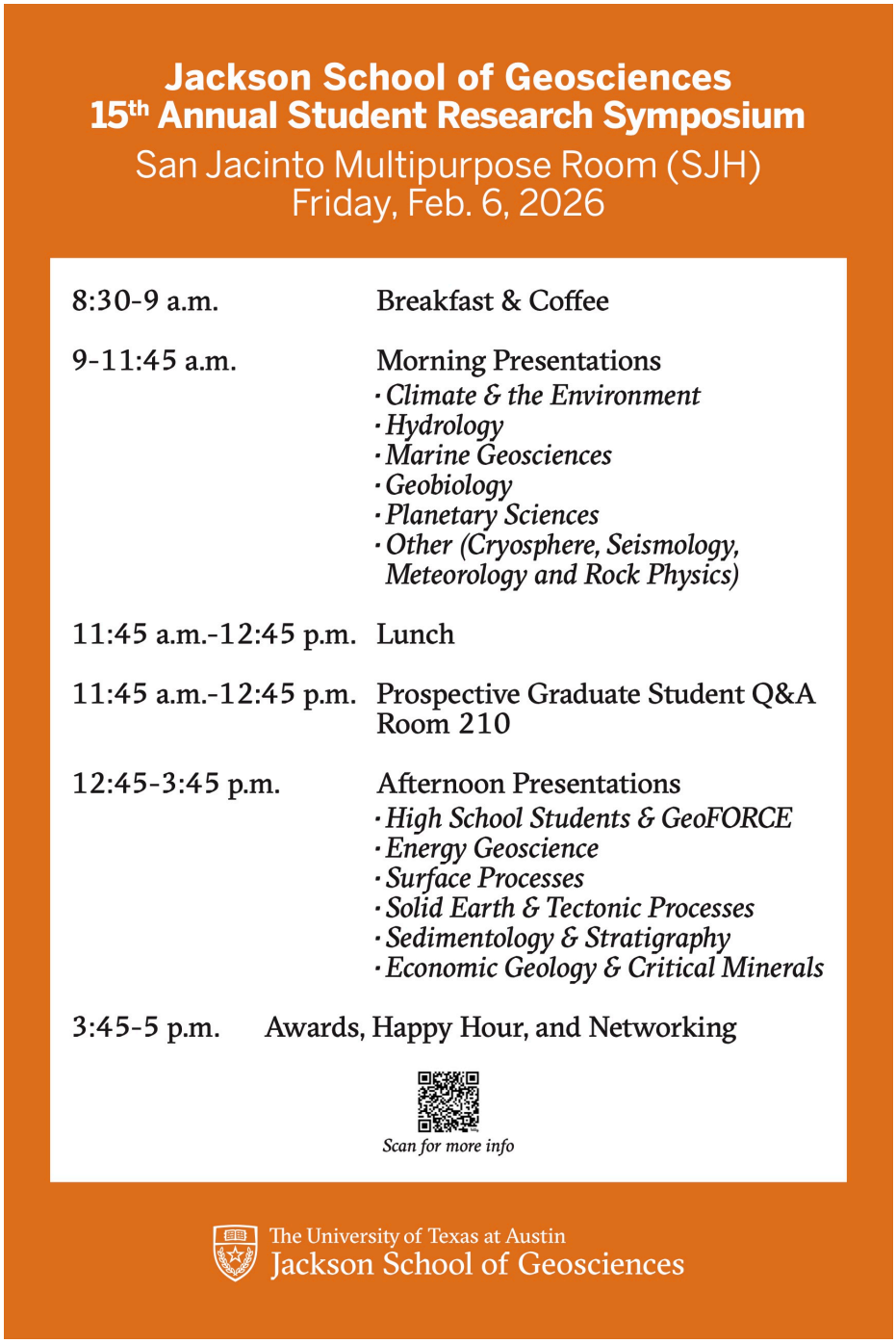

Map of Booth Numbers

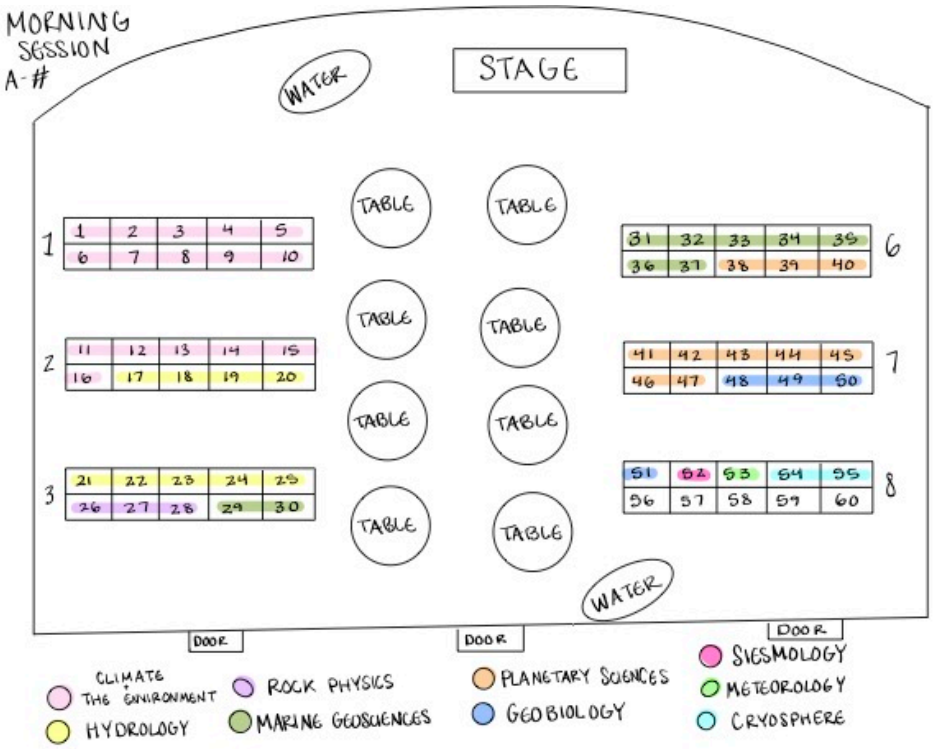
MORNING SESSION
A-#
STAGE
WATER
TABLE
1 1 2 3 4 5 6 7 8 9 10
2 11 12 13 14 15 16 17 18 19 20
3 21 22 23 24 25 26 27 28 29 30
6 31 32 33 34 35 36 37 38 39 40
7 41 42 43 44 45 46 47 48 49 50
8 51 52 53 54 55 56 57 58 59 60
WATER
DOOR
DOOR
DOOR
CLIMATE + THE ENVIRONMENT
ROCK PHYSICS
PLANETARY SCIENCES
SEISMOLOGY
HYDROLOGY
MARINE GEOSCIENCES
GEOBIOLOGY
METEOROLOGY
CRYOSPHERE

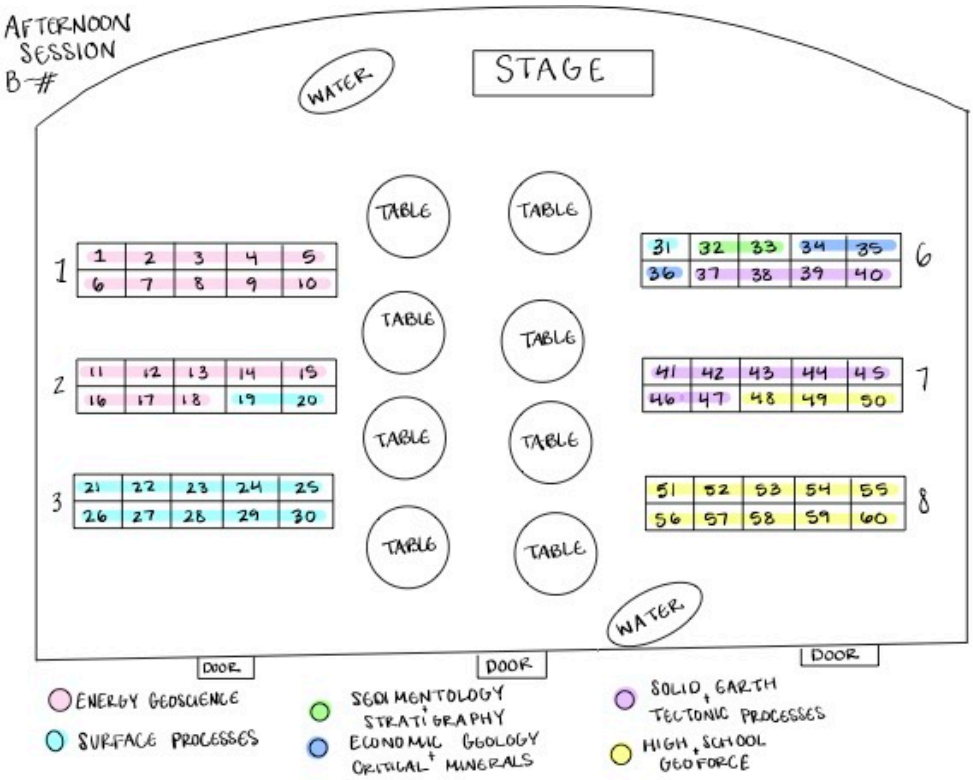
AFTERNOON SESSION
B-#
STAGE
WATER
TABLE
1 1 2 3 4 5 6 7 8 9 10
2 11 12 13 14 15 16 17 18 19 20
3 21 22 23 24 25 26 27 28 29 30
6 31 32 33 34 35 36 37 38 39 40
7 41 42 43 44 45 46 47 48 49 50
8 51 52 53 54 55 56 57 58 59 60
WATER
DOOR
DOOR
DOOR
ENERGY GEOSCIENCE
SEDIMENTOLOGY + STRATIGRAPHY
SOLID EARTH + TECTONIC PROCESSES
SURFACE PROCESSES
ECONOMIC GEOLOGY + CRITICAL MINERALS
HIGH SCHOOL + GEOFORCE

Index

Morning Session: 9:00am – 11:45am

Climate & The Environment (16 Participants)

Lee, Chieh-Chen; Yang, Zong-Liang; Hu, Chenxi; Wu, Zhaohua

"Integrating Multi-Scale Empirical Mode Decomposition to Elucidate Spatio-Temporal Changes of Extreme Precipitation in the Colorado River Basin, Texas"

Booth #A-1

This study analyzes historical and projected changes in extreme precipitation across the Colorado River Basin (CRB), a key water source for Austin, Texas. We combine high-resolution European Centre for Medium-Range Weather Forecasts fifth generation (ERA5) reanalysis data (0.25° × 0.25°) with future projections from five top-performance Coupled Model Intercomparison Project Phase 6 (CMIP6) global climate models (GCMs). Our goals are (1) detecting spatial and temporal trends in annual precipitation, maximum 1-day (Rx1day) and 5-day (Rx5day) rainfall, and dry-day frequency, and (2) assessing future changes in extreme rainfall intensity and frequency.

Linear historical trends in ERA5 are estimated using ordinary least squares regression. To uncover nonlinear, multi-decadal patterns, we apply Empirical Mode Decomposition (EMD). Spatial analysis reveals three distinct patterns: (1) intensifying short-duration extremes (Rx1day, Rx5day) upstream, (2) increasing drought frequency (more dry days) in the upper basin, and (3) rising annual precipitation totals downstream. EMD reveals low-frequency (e.g., quasi-decadal) cycles not captured by linear methods. We use the mask-EMD approach to extract intrinsic mode functions (IMFs) from each grid cell, then group them into high (IMF1–4), medium (IMF5–7), and low-frequency (IMF8) bands to isolate weather-scale to decadal signals. The mid-basin shows strong high-frequency variability linked to wetter conditions, while the upper basin is dominated by long-term drying trends. For future extremes, we fit Generalized Extreme Value (GEV) distributions to Rx1day. Under the SSP5-8.5 scenario, current 100-year precipitation events may occur 2-3 times more frequently by the late century. Our findings reveal an urgent adaptation imperative that the CRB's spatially divergent projected precipitation extremes require immediate implementation of differentiated infrastructure strategies, from enhanced flood defenses mid-basin to drought-resilient systems upstream, to protect residents and critical water resources.

Johnson, Tanner; Touma, Danielle; Johnson, Joel; Rempe, Daniella

"Using machine learning to evaluate climatic controls on wildfire severity across the western United States"

Booth #A-2

Associated with a warming global climate, wildfire area and severity are expected to increase across western North America. High-severity burns are particularly destructive to landscapes and can lead to hazardous post-fire events such as debris flows and flash floods. In this study, we aim to quantify how wildfire severity is influenced by interactions among drought, fire weather conditions, and fuel characteristics. Using the Monitoring Trends in Burn Severity (MTBS) dataset, we identify low, moderate, and high severity burn areas from 1984 to 2024. We pair these fire records with meteorological, fuel, and climate variables from gridMET to assess potential drivers of severity. We also investigate spatiotemporal patterns in fire severity, burned area, and climatic drivers across EPA Level III Ecoregions. Our results show that the total area burned at high severity across the western U.S. increased substantially from 1984–2003 to 2004–2024, with the largest increases observed in the Cascades (952.3%), Sierra Nevada (288.5%), Klamath Mountains (359.4%), and the Northern Basin and Range (98%). Similar upward trends were observed for area burned at low and moderate severities. Southern California was the only region that experienced a substantial decrease in area burned at high severity (-68%). We then assessed the climatic and meteorological drivers of low, moderate, and high-severity wildfires using random forest regression (RFR) methods over the 41-year period. The RFR ability to predict fire severity varied regionally and seasonally, with the Southern California/Baja region performing the best for low severity fires during the winter months ($R^2 = 0.69$). The Sierra Nevada region 2 produced the best performing RFR for fires burned at high and moderate severity ($R^2 = 0.35$). For predicting moderate and high severity burned areas, standardized vegetation index and minimum relative humidity were the most important variables. However, wind speed emerges as a key feature for high severity burned areas. Our findings enhance the ability to predict wildfire severity and provide valuable insights for operational applications such as wildland fire management, emergency preparedness, and fire forecasting.

Bautista, Sophia; Shanahan, Tim; Augustinus, Paul

"Understanding the Orbital to Millennial-Scale Variability of the Southern Hemisphere Westerly Winds: Biomarker Reconstructions from the North Island of New Zealand"

Booth #A-3

From heat transfer to storm regulation, the Southern Hemisphere westerly winds (SHWW) play a key role in the global climate by balancing climate perturbations between the high and low latitudes. On glacial timescales, the latitudinal position of the SHWW has major implications for Southern Ocean CO 2 storage, making them an essential feedback mechanism for past changes in global climate. While studies have suggested that the westerlies vary in position and intensity in response to orbital and millennial-scale forcings, climate models and proxy data disagree about the nature of

the SHWW responses to orbital forcings and glacial boundary conditions. Our knowledge of the SHWW is further limited due to the lack of well-dated, unambiguous proxy indicators. To address these uncertainties, we generated a continuous 130-kyr long, high-resolution proxy reconstruction of the SHWW from Orakei Basin and Lake Pupuke, located on the North Island of New Zealand, using the hydrogen isotope composition of sedimentary leaf waxes as a proxy for Southern Hemisphere moisture sources associated with changes in the position of the SHWW. We complement these data with temperature reconstructions using the MBT' 5ME index. The temperature record shows a rapid cooling of 3 o C transitioning out of the Eemian, then remains relatively stable throughout most of the last glacial, with minimum temperatures centered on ca. 70-ka and during the Last Glacial Maximum. On orbital timescales, temperature and dD wax variations are broadly synchronous with Antarctic temperature changes, reflecting the influence of large-scale, global climate processes on the position and strength of SHWW. However, on millennial timescales and during the deglaciation, their agreement weakens, suggesting important differences in the controls of the SHWW and temperature on these timescales. These findings highlight the complex, time-scale dependent nature of the SHWW, emphasizing their role in modulating regional hydroclimate and contributing to global climate feedbacks across glacial-interglacial timescales.

Ojo, Gabriel; Lowery, Christopher; Martindale, Rowan; Sylvester, Zoltan

"Tracking Changes in the South Atlantic Subtropical Gyre Over the Last 6 Mya using Planktic Foraminifera"

Booth #A-4

The South Atlantic Subtropical Gyre (SASG) is a major component of the Atlantic Meridional Overturning Circulation (AMOC) and strongly influences regional stratification, nutrient distribution, and carbon cycling across hemispheres. Although modern satellite observations show the SASG is migrating poleward and changing in strength under ongoing climate warming, the long-term natural variability of the SASG remains poorly understood. Reconstructing its response to past climate transitions is essential forevaluating the role of the SASG in regulating ocean circulation and ecosystem structure.

This study presents a preliminary assessment of planktic foraminiferal ecology, X-ray Fluorescence (XRF) proxy measurements, and machine-learning-based test-size variation over the last ~6 myr at IODP Site U1559, located in the central South Atlantic. We analyzed 20 core samples and classified assemblages into respective ecological groups based on depth habitat and trophic strategy (i.e., mixed-layer symbiont-bearing, mixed-layer non-symbiont, thermocline, subthermocline, and high-latitude ecogroups). We found all five ecogroups in varying proportions, with mixed-layer assemblages

dominating the Late Miocene-Pliocene interval when surface conditions were warmer, followed by a shift toward thermocline and sub-thermocline assemblages during the Pleistocene as global cooling increased stratification and expanded thermocline habitats. During this cooling, peaks of high latitude taxa are commonly observed suggesting incursions of subpolar waters into the SASG. Variations in the shell size of Globigerina bulloides were analyzed using 'segmenteverygrain', a machine learning algorithm for image segmentation of grains but herein adapted for planktic foraminifera. The variations in the shell size of G. bulloides suggest sensitivity to changing nutrients and water-column structure. XRF elemental data for terrigenous input (i.e., Fe/Si ratio) roughly parallels the size variation of this opportunist taxa, providing evidence for dust-driven terrigenous fluxes into the SASG, notably during the Late Miocene, and middle Pleistocene interval.

These initial results indicate that long-term cooling has driven major reorganizations in upper-ocean hydrography and ecological community structure within the SASG. Future work is focused on expanding our sampling resolution to capture short-term climate variations, stable isotope analysis, and species-specific size analysis. These data will provide the first multi-proxy record of the SASG evolution across major late Cenozoic climate transitions and offer insights relevant to predicting SASG behavior under continued anthropogenic warming.

Reich, Shoshi; Aretz, Nicole; Wilcox, Karen; Heimbach, Patrick

"Data-driven reduced-order modeling for a double-gyre ocean using operator inference"

Booth #A-5

Numerical ocean models are powerful tools for simulating ocean circulation, but their high computational cost can be limiting. This poses a major challenge for tasks like uncertainty quantification or sensitivity analyses, which require many forward model evaluations. To address this, we develop reduced-order models (ROMs) as efficient surrogates that can be used to analyze ocean response to a range of atmospheric forcing conditions. Our approach is data-driven and leverages the Operator Inference framework to learn low-dimensional dynamical systems from high-fidelity simulation data. Operator Inference combines data-driven learning and physics-based modeling by learning the reduced operators that minimize the misfit between projected state snapshots and reduced dynamics. While the method has shown success in systems with low-dimensional parameter spaces and relatively simple forcing functions, ocean models present notable challenges; they often exhibit slow eigenvalue decay in proper orthogonal decomposition and are driven by complex, spatially and temporally varying forcings that are major drivers of ocean circulation. To address these difficulties, we utilize a parallelized version of OpInf that ensures the ROM remains computationally efficient while accurately capturing the system's behavior. We apply this methodology to a double-gyre ocean

subject to time-varying wind and buoyancy forcing in a fully three-dimensional spatial domain. Results show that the learned ROM achieves low prediction error and substantial computational speedup, demonstrating the potential of Operator Inference for enabling fast and reliable ocean simulations that can be used for climate predictions under a range of forcing scenarios.

Hartmetz, Anna-Elizabeth; Shanahan, Timothy; Anderson, R. Scott

"Insights into the Deglacial in Southwestern North America from a Lacustrine Record in Northeastern Arizona"

Booth #A-6

During the last glacial maximum, southwest North America was wetter than the present, and as deglaciation progressed, shifts in the seasonal precipitation regimes occurred. However, the relative contribution of summer and winter precipitation, as well as their underlying mechanisms and forcings remain uncertain because long continuous paleoclimate records from this region are relatively rare. Here, we present a new reconstruction of past climate changes spanning the past ca. 45,000 years from Potato Lake on the Mogollon Rim in northeast Arizona using leaf wax δD and branched glycerol dialkyl glycerol tetraethers. Paleotemperatures estimated using the MBT'5Me index show ca. 6.5℃ of cooling during the last glacial, and an early Holocene thermal maximum that is ca. 1℃ warmer than the preindustrial. Deglacial warming occurs gradually and starts early, beginning at immediately after the last glacial maximum (LGM) at ca.21-22 ka. A slight cooling of ca. 1℃ occurs synchronously with the Younger Dryas stadial. In contrast, δDwax values peak during the LGM, but do not change significantly until ca. 16.3 ka, when they decrease abruptly. The differences between the δDwax and temperature reconstructions suggests a decoupling between temperature and atmospheric dynamics during the deglacial, reflecting differences in the underlying processes driving precipitation and temperature changes at that time.

Brooks, Trevor; Subharsan, Naveen; Kamath, Harsh; Niyogi, Dev

"Austwin: An Urban Heat Digital Twin for Austin Texas"

Booth #A-7

Urban heat presents a growing challenge for cities, with localized Urban Hot Spots (UHS) amplifying risks to human health, infrastructure, and energy systems. This study introduces the AusTwin, a digital twin of Austin, Texas, developed to simulate and analyze extreme heat at high spatial and temporal resolution and allow for the city to make long term decisions. AusTwin employs the Universal Thermal Climate Index (UTCI) as its core metric, enabling comprehensive assessment of human thermal stress by integrating air temperature, humidity, wind speed, and radiation. The platform can

help identify UHS by examining a multitude of factors (meteorological data, energy data, POI data, and social science data). Through scenario modeling, AusTwin evaluates the potential impacts of adaptation strategies, including urban greening, reflective pavements, and shading interventions, on reducing thermal stress. By coupling physical and human-centered indicators of heat, the AusTwin provides a framework for advancing urban climate research and supporting evidence-based decision-making. This DT demonstrates the utility of human based modeling and data collection for diagnosing UHS and assessing the effectiveness of adaptation strategies in mitigating extreme heat exposure.

Dallmann, Allysa; Davis, Braniff; Niyogi, Dev

"Data Drive Decisions - A framework for understanding how cities utilize meteorological data in their operations."

Booth #A-8

There has been ongoing risk from natural hazards, accompanied with vagaries in weather patterns. With the infrastructure risk, insurance costs, and economic stakes on the rise, there are heightened concerns for disaster awareness and preparedness especially as it relates to cities. From the meteorological perspective, there are many open-source data, products, and tools that are typically available. However, with the inundation of access to information there is also a paradoxical paucity of data that is relevant to the actual operations and decision, amidst challenges such as data quality, volume, credibility, what is allowable to be used in operations, especially on the local to city level. There is also the question of what new data or analysis of datasets needed or will be in alignment with city projects, and decision-making. This research addresses the above topic by focusing on the decision-making process for the City of Austin regarding meteorological information and data use in departmental operations. This specific presentation will focus on the operations of Austin Fire Wildfire Division. We conducted a series of focus group studies and workshops, leveraging the UT-City Colab and for prescribe burn operations. From this analysis, we found that there is a need for mapping data with decisions and to develop a framework for this process. There also is a need for the localization of atmospheric datasets that can be used for effective dataset development, localization of information, and translating data to decisions. Accessibility of this information would aid in developing local risk tools and aid in preparation and planning.

Seiner, Owen; Halberstadt, Ruthie; Keisling, Benjamin

"Diagnosing Saddle Instability: A Lyapunov Approach to Ice Sheet Separation"

Booth #A-9

Geometrical-dynamical instabilities are recognized as critical drivers of ice sheet stability, with the potential to trigger nonlinear sea-level fluctuations from relatively small climate forcings. A prime example is Meltwater Pulse 1A (~14.6 kyr) where global sea levels rose 10–20 m in roughly 500 years (rates of centimeters per year, compared to contemporary millimeters per year), an event linked to the collapse of the saddle connecting the Laurentide and Cordilleran ice sheets. In this study, we combine ice sheet model simulations of idealized, randomly generated saddle geometries with a Lyapunov-like stability functional to analyze the dynamical signature of this collapse. We demonstrate that the onset of instability is governed by a local energetic tipping point; collapse initiates when the stabilizing sensitivity of power dissipation to thickness changes falls below the magnitude of the destabilizing surface mass balance feedback. This criterion successfully predicts the onset of runaway thinning and flow reorganization, providing a quantitative framework to identify the initiation of similar bifurcations in both paleo-records and future projections.

Mallesh, Rakshith; Niyogi, Dev; Okumura, Yoko; Guan, Bin

"Rivers in the Sky: Why do they prefer to form over Texas?"

Booth #A-10

Atmospheric Rivers (ARs) are narrow, river-like streams in the atmosphere with an intense concentration of water vapor. ARs are generally found in midlatitude regions, and can cause rainfall and flooding when they intercept land regions. At the same time, they are essential for water security in regions like California, where it contributes to as much as 50 percent of the annual rainfall. Because of this, most of the existing literature focuses on ARs affecting the west coast of the US, even though many of them affect the east coast and the interior continental US.

A closely related, open question is related to the following observation: the global AR generation frequency map has 3 major hotspots, all over subtropical land areas. This includes the southeastern United States and the region centered around Texas. These areas are located near the southern side of subtropical westerly jets and largely correspond to the entry locations of midlatitude storm tracks. The reason for the higher AR genesis frequency over land than the ocean remains unclear. We investigate the causes for enhanced AR genesis over Texas. Results indicate that ARs prefer to form over land, with a possible role of surface heating and latent heat fluxes from surrounding oceans. The role of El Nino and the seasonality of genesis is also studied.

Kamath, Harsh; Patel, Aditya; Sudharsan, Naveen; Yang, Zong-Liang; Niyogi, Dev

"Thermal Comfort Path Planning for Urban Mobility in Austin, Texas"

Booth #A-11

This study demonstrates an application of SOLWEIG-GPU in developing walking and biking path planner that provides optimal thermal comfort for Austin, Texas. Using GPU-accelerated simulations, we created a city-scale Universal Thermal Climate Index (UTCI), allowing us to examine differences in heat stress at meter-level resolution based on urban geometry, vegetation, and micro-meteorological conditions. This high-resolution thermal comfort data was are utilized in conjunction with routing data obtained from the Google Maps API to evaluate walking paths based on thermal comfort. Each path takes into account multiple factors, such as cumulative heat exposure, topography, length and shade, ultimately creating suggested paths with maximum shade & minimum thermal discomfort that a user could take from origin to destination. This study outlines our application of the GPU accelerated SOLWEIG model as a proof of concept to further encourage enhancements to urban mobility planning, and provide an applied decision-support system to assist heat stress management for building resilience in hotter cities.

Hozven, Fletcher; Touma, Danielle; Persad, Geeta; Stevenson, Samantha; Pfleger, Cali

"Still Dry After the Drought: Modeling Soil Moisture Recovery in the Colorado River Basin"

Booth #A-12

Drought in the Southwestern United States is projected to intensify over the next few decades, to the point where conditions considered a drought today are expected to become average. As this "new normal" sets in, declaring drought conditions is becoming a great challenge. Previous literature has focused on drought intensity and lifespan rather than post-drought conditions. We use volumetric soil moisture, a widely used proxy for assessing drought conditions, to address this gap and ask: Will future drought recovery periods return soil moisture to the historical norm, or will the droughts "end" at significantly drier levels? Using the Community Earth System Model 2 - Large Ensemble (CESM2-LENS) at the high-emissions scenario and ERA5 reanalysis data, this study analyzes projected drought conditions in the Colorado River Basin. Our findings show that in the 21st Century, drought recovery periods do not return soil moisture to the historical normal and "end" at significantly drier levels. The Colorado River Basin is transforming rapidly and the soil moisture percentiles in our historic normal do not represent the equivalent soil moisture values today. This research provides insight into water management and societal implications as droughts become less likely to recover.

Risinger, Hannah; Niyogi, Dev

"Using MRMS Data and the Weather Research and Forecasting model to Identify Precipitation Patterns in the Austin Area"

Booth #A-13

Urban environments can significantly influence convective processes, altering precipitation patterns. This study will use the high-resolution Multi-Radar Multi-Sensor (MRMS) dataset to study the storm modifications in and around Austin, Texas. The MRMS dataset has a spatial resolution of 1 km, temporal resolution of 2 minutes, and 3D mosaics at 31 vertical levels that spans from 2020 to 2025 making it uniquely suitable for studying small scale urban storm modifications. The study will identify all the storms that occurred around Austin, from 2020 to 2025, by considering the rainrate, rain area, and rainfall duration. Composite structures of storm characteristics like intensity, duration, and diurnal patterns will be prepared, giving us an insight into the storm behavior around the City of Austin. Characterization of vertical storm profiles before, during, and after convection will be shown, along with different storm behavior associated with various types of convection. The Weather Research and Forecasting (WRF) model will be used with a 9-3-1 km resolution nested domain setup, to simulate a number of representative storms. The best performing model simulations will be used to analyze atmospheric diagnostic parameters such as convective available potential energy (CAPE), convective inhibition (CIN), moist static energy, and Theta E profiles. Understanding these characteristics of how storms behave around the city will help cities design better flood response mechanisms and improve current storm prediction models.

Maruri, Philip; Sudharsan, Naveen; Niyogi, Dev

"An Analysis of the Historical Dynamics of the Urban Heat Island in Austin, Texas"

Booth #A-14

Extreme heat presents a growing threat to urban areas. Austin, Texas, as a rapidly developing city in the increasingly hot sunbelt region, is particularly vulnerable to this threat. This study analyzes daily meteorological records, both observation and reanalysis, in relation to satellite data to understand the growing risk of extreme urban heat in the city and to better inform policymakers. Historic temperature data is analyzed to characterize the transformation of the city's urban heat island (UHI) effect over the past four decades, with analysis focusing on long-term trends, seasonal dynamics, and diurnal characteristics. The UHI signal is explored in relation to land-use changes in Austin and long-term climate change. Analysis reveals that Austin's heat island, while mild, is growing with time, especially in daytime hours. Intensity is greatest in the autumn and spring. Strong correlation exists at a year-by-year resolution between fractional impervious surface differences and UHI signal, suggesting that growth in UHI signal is likely driven by urbanization.

Janelle, Alexander J.; Rocha, Michael; Banner, Jay L.; Miller, Nathaniel R.; Gunna, Heather

"Regionally extensive mineral-solution reactions in karst: Insights from modern cave monitoring and seasonal trace element variations during the last deglacial"

Booth #A-15

Trace elements in speleothems are widely used as a paleoaridity proxy. This proxy is based on the relationship between a common mineral-solution reaction in the vadose zone, prior calcite precipitation, the extent to which vadose pore spaces are saturated, as a result of hydroclimatic moisture input. There are, however, multiple other mineral-solution reactions common to the karst vadose zone (epikarst), including water-rock interaction (i.e., incongruent dissolution, congruent dissolution, and recrystallization) that also influence trace element behavior in drip water and their eventual incorporation in speleothem calcite. Paleoaridity interpretations based on trace element variations that conflate the controls of these mineral- solution reactions will introduce inaccuracies. To address this, we conducted an integrated analysis of Sr isotopes and trace elements in multiple caves systems on a regional scale as a means to differentiate between these reactions.

We present seasonally-resolved cave monitoring data, including drip-water trace element and isotopic composition, cave atmospheric conditions, and plate calcite growth and trace element composition from four caves spanning 300 km across the Edwards Plateau in central Texas, USA. For one of these caves, we present element maps for a late Pleistocene stalagmite that display high-resolution trace element couplets consistent with seasonal banding. We use these time series data and modeling of mineral-solution reactions to distinguish between the mechanisms controlling drip-water trace element variations. Physical flow data for the drip sites indicate a spectrum of diffuse- to conduit-flow paths for drip waters. A correspondence between physical flow path type and geochemical variations provides evidence for specific mineral- solution reactions affecting drip-water composition. Across locations and sites within a location, water-rock interaction sets the baseline trace-element signal by governing the initial reaction progress, while prior calcite precipitation diverts geochemical evolution pathways from this baseline, in response to seasonal ventilation-driven variations in epikarst pCO_2. Drip sites in all four caves show similar extents of water-rock interaction and similar geochemical divergence points for prior calcite precipitation, suggesting a regional control on maximum pCO_2 conditions in the epikarst. In the context of the stalagmite seasonal trace element couplets, this suggests a consistency of mineral-solution reactions across the Edwards Plateau during the last deglacial.

Our findings emphasize the insight provided by 1) modern cave monitoring for speleothem paleoclimate interpretations and 2) integrating Sr isotopes into trace element studies. We demonstrate regional consistency in the controls of trace-element behavior across a karst system in the modern and late Pleistocene. These findings highlight the regional role of CO_2 dynamics in the karst critical zone and its bearing on paleoclimate interpretations from speleothem proxies.

Shank, E. M.; Donaldson, Amanda; Rempe, Daniella

"Evaluating the relationship between tree size and drought sensitivity across a storage capacity gradient"

Booth #A-16

Multi-year droughts impact Mediterranean montane forest productivity, yet nearby forests often show contrasting growth responses to similar climatic conditions. Root-zone moisture storage has been hypothesized to mediate drought vulnerability at both forest stand and tree scales. At the stand scale, high bedrock storage capacity may buffer forests by banking subsurface moisture across years. At the tree scale, larger trees with more extensive root systems may access greater moisture volumes. We hypothesized that if both factors enhance water availability, large trees would show less growth reduction during multi-year droughts than small trees, particularly at high-storage sites. Alternatively, if high-storage sites accumulate substantial moisture deficits during multi-year droughts, this site-level deficit may negatively impact tree growth regardless of size. To address these hypotheses, we analyzed tree-ring width indices (RWI) from three Sierra Nevada pine forests within 4.5 km that experience identical climate forcing but have contrasting root-zone storage capacities (291, 608, and 1027 mm). At each site, we sampled trees across a similar size distribution and divided samples into small versus large size classes (n = 8-9 trees/class/site) based on site median diameter at breast height (64-66 cm). Within a site, results show similar growth trajectories between large and small trees, suggesting comparable productivity between size classes. However, during California's 2012-2015 megadrought, the highest-storage site experienced the greatest growth reduction, consistent with storage deficit carryover creating site-level deficits impacting both size classes. These findings demonstrate that site-level subsurface storage deficits can mediate forest drought vulnerability independent of tree size, with important implications for predicting and managing forest drought responses.

Hydrology (9 Participants)

Mukherjee, Neelarun; Gao, Bo; Coon, Ethan; Shuai, Pin; Hill, Devon; Nielson, Bethany; Cory, Rose; Kling, George W; Chen, Jingyi; Cardenas, M. Bayani

"Hydrologic and thermal changes in supra-permafrost soils and aquifers over the last four decades of warming"

Booth #A-17

The climate record from the last four decades (1981-2020) shows that the North Slope of Alaska has experienced rapid increase in winter air temperatures by up to 3.5 o C and snowfall increasing by ~40 mm. These shifts are altering not only surface energy balances but also the thermal and hydrological states of the soils and shallow aquifers above permafrost. These supra-permafrost aquifers (SPAs) have high concentrations of dissolved organic carbon (DOC) leaching rapidly from peat, the main SPA material. The

transport of DOC into aquatic water bodies and biogeochemical transformation into CO 2 and CH 4 depend on thermal and hydrologic conditions. However, the hydro-biogeochemical responses of SPAs to long-term climate are largely unknown. In this study, we combined high-resolution, high-fidelity modeling using the Advanced Terrestrial Simulator (ATS) to evaluate 40 years of climate impact on the thermal regime, groundwater flow, and DOC transport across a representative hillslope-riparian transect in the Imnavait Creek watershed a typical headwater region on the North Slope. We combined long term and specific year-long meteorological, land-surface and subsurface observations for model calibration, followed by long term ATS simulations using historical meteorological forcings. Rising winter air temperatures and snowfall have led to increased annual outflow from the hillslope-riparian zone to the creek as well as warmer soil temperatures in winter, more extensive zero-curtain zones (subsurface locations where soil temperature hovers near 0 o C due to latent heat exchange during freeze/thaw) and longer zero-curtain periods. The model showed that in 2018 the zero curtain extended into the typical coldest day of the year (January 22), when up to 180 days of zero curtain period was observed near the riparian zone. This situation would allow for sustained liquid water saturation with negligible subsurface flow as well as microbial activity deep within the cold season. Our findings provide insight on the mechanisms driving high early spring and late winter greenhouse gas emissions from the SPA. This work shows that there may be more hydrological activity in the Arctic winter at this site that previously thought, which could drive enhanced carbon emissions under future climate.

Davis, Hudson Finley., Cardenas, Bayani

"Analysis of Well Depths from 1920-2023 for the Major Aquifers of Texas"

Booth #A-18

This study investigates long-term trends in depths of wells drilled for the nine major Texas aquifers from the period of 1920 to 2023. Analyses of these data through various statistical methods suggest that all but one of these aquifers show sustained deepening of well-depths from 1920 to 2023, which likely indicates and is a result of long-term groundwater depletion and water-level deepening. However, upon narrowing the time range to more recent years, it is revealed that more than one aquifer has experienced shallowing well-depths in recent times, likely indicating that localized recovery (recharge) of groundwater resources could be occurring in some areas. These patterns have significant implications for the future of water security in the state of Texas. Persistent over-exploitation of groundwater resources, driven by factors such as prolonged drought, expansion of irrigated agriculture, and population growth, poses substantial risks to municipal water supply, agricultural production, and ecosystem stability statewide. Through the analysis of an extensive historical dataset where well

depth values act as an indirect proxy for groundwater level, this study highlights regions in Texas in which groundwater availability may have declined, most notably the regions that overlie the Ogallala and Edwards-Trinity Plateau Aquifers. These results show that in many places across Texas, residents likely need to drill deeper to extract groundwater.

Gomes, Talita., Matheny, Ashley

"Hydrologic Connectivity and Mangrove Resilience in a Tropical Coastal System"

Booth #A-19

Mangroves are an efficient coastal ecosystem that provides key ecosystem services in tropical and subtropical regions. They stabilize shorelines, reduce storm surge, sequester carbon, regulate nutrient cycling, and serve as essential habitat for diverse marine and terrestrial organisms. In the Caribbean, mangrove systems are threatened by anthropogenically altered freshwater input, climate variability, and extreme events. These mangroves play a role in maintaining coastal water quality and ecosystem stability, especially in hydrologically complex environments such as the Luminous Lagoon, a bioluminescent system influenced by freshwater discharge, groundwater inputs, and tidal exchange. The lagoon receives freshwater from the Martha Brae River, where the hydrology directly affects salinity gradients, nutrient delivery, and mangrove stress along the lagoon fringe.

My PhD investigates how hydrologic connectivity across the watershed–mangrove–coastline controls mangrove function and resilience. The research is structured around three projects. Project 1, quantifies groundwater–surface water interactions along the Martha Brae River and its discharge to the coastal zone using radon, water quality parameters, and nutrient analyses. Project 2, focuses on mangrove ecohydrology along the Luminous Lagoon, examining how hydroclimate variability and freshwater–marine mixing regulates mangrove water use, physiological stress, and growth. Project 3 evaluates mangrove damage and recovery after Hurricane Melissa 2025 using remote sensing and GIS-based analyses. LiDAR, bathymetry, and Normalized Difference Vegetation Index time series are integrated to map changes in mangrove structure, coastal morphology, and vegetation recovery trajectories.

By linking watershed hydrology, mangrove ecohydrology, and landscape-scale disturbance response, this research advances our ability to predict mangrove vulnerability and recovery under changing climate and hydrologic regimes.

Nguyen, Amber., Cardenas, Bayani., Williams, Ebony., Cortazar-Cepeda, Mario

"Seawater-Groundwater Mixing Dynamics in a Groundwater-fed Estuary: Ría Celestún, Yucatán, Mexico"

Booth #A-20

Estuaries, due to their unique mixing dynamics, are vital habitats for animals and fisheries, which are the economic backbone for many coastal communities through tourism and natural resources. However, they are threatened by climate change and development. While estuaries are commonly supplied with freshwater input from rivers, groundwater-fed estuaries possess distinct mixing dynamics that have been less studied. Ría Celestún, in Yucatán, Mexico, is a groundwater-fed estuary heavily impacted by human activity, notably a bridge that intersects the center. This research aims to explore the physical and chemical mixing dynamics of Ría Celestún. Specifically, this research addresses the following questions: 1) How does the extent of groundwater and seawater mixing of Ría Celestún change seasonally? 2) How far in does the tide penetrate in Ría Celestún, and how does its behavior change seasonally (considering the seasonal shift in sea level)? and 3) How much does the chemistry change along the estuary, and how is this connected with changing groundwater inputs? To answer questions 1 and 3, we gathered transect and individual sample water quality data from three different months: May 2024, December 2024, and March 2025. To answer question 2, we collected around 24-hour cycle transducer data for the same three months. Preliminary data show that the estuary is saline in the summer, becomes fresher in the winter, and goes to an intermediate stage in the spring. Future work will use these field-collected data to train a model and predict the estuary's overall temporal behavior. The outcomes of this research will help establish the hydrological behavior of Ría Celestún and provide insights into similar estuarine systems. By advancing our understanding of seasonal mixing dynamics, these findings can guide the management and conservation of these critical habitats.

Chou, Trinity; Pinzon, David Bahamon; Banner, Jay

"Tracing supply and wastewater leakage in Austin, Texas, through emerging contaminants and microbial indicators"

Booth #A-21

In rapidly urbanizing areas like Austin, Texas, it is increasingly important to preserve water resources and utilize them in sustainable ways. In a state that is projected to face increased drought severity and frequency in the later 21 st century, assessing water quality in urban areas is crucial. While leakage and failure in both supply water and wastewater networks contribute to altered urban watershed hydrology, wastewater leakage poses a particularly significant human health risk due to exposure to emerging contaminants and pathogenic bacteria. However, the presence of these contaminants and microbes within wastewater make them especially suitable tracers for contamination in surface water. This research aims to quantify the extent and pathways of wastewater leakage in Austin, Texas by employing traditional water quality parameters (cations and anions), microbial indicators (e.g., Escherichia coli), and emerging contaminants (PFAS, pharmaceuticals, and artificial sweeteners). Stream water samples will be collected from

watersheds with varying levels of urbanization and the Colorado River, as well as drinking water and wastewater samples from Austin's municipal network. Fluid mixing modeling will be employed to quantify the proportion of wastewater contributing to Austin watersheds. Preliminary data from previously collected samples show higher concentrations of contaminants, E. coli, and wastewater-associated ions (e.g., NO 3 and PO 4) in urban sites. A trend in the Colorado River was observed where PFAS, emerging contaminant (carbamazepine, sulfamethoxazole, sucralose), and wastewater-associated ion concentrations increased downstream in the river, coinciding with wastewater treatment plant locality. A sharp increase in PFAS concentrations was also observed at a rural site downstream of the Austin airport.

Khojeh, Shokoufeh (Shuku)., Sui, Xinxin., Tavakoly, Ahmad Ali., Yang, Zong-Liang

"Event-Based Analysis of Urbanization Effects on Precipitation in Texas"

Booth #A-22

Urbanization alters land-atmosphere interactions and has been increasingly linked to changes in precipitation characteristics; existing evidence generally suggests that urban areas are getting more total rainfall compared to rural areas based on temporally aggregated precipitation metrics. However, precipitation is an intermittent and discontinuous process that occurs by independent events. Because urban flooding and infrastructure impacts are driven by individual rain events-particularly short-duration, high-intensity storms-an event-based framework is essential for understanding urban precipitation responses. To address this important knowledge gap, here we employ hourly satellite-based precipitation data and an event-based rainfall analysis over cities in Texas during 2001-2024. Rainfall events are identified using a Minimum Inter-Event Time (MIET) approach, allowing storms to be separated based on dry intervals rather than fixed time windows. Storm properties including intensity, duration, volume, frequency, and inter-event variability are quantified and compared between urban and surrounding rural regions. Results showed that across Texas cities, urban areas generally experience higher storm intensities and volumes than their surrounding areas, with approximately 82% of cities showing larger storm volumes and 91% exhibiting stronger storm intensities. These findings highlight the importance of event-based analyses for diagnosing urban precipitation changes and provide new insights into how urbanization reshapes storm intensity and hydrologic risk under ongoing urban expansion.

Libbing, Sydney., Banner, Jay., Clamann, Andrew., Porras, Abel

"Titanium from Reflective Pavement in Austin-area Streams: Urbanization Impacts and Implications for Climate Resilience Planning"

Booth #A-23

Urban Stream Syndrome affects several streams in Austin, Texas, where recent and rapid development characterized by expanding impervious surfaces within watersheds is altering stream hydrographs and pollutant loading, leading to growing concerns about water quality, urban heat, and ecosystem health. One climate resilience strategy gaining attention is the use of reflective pavement sealants, which contain titanium dioxide (TiO_2) to reduce urban heat through increased reflectivity. While pilot programs show cooling effects, the environmental fate and ecological risks of TiO_2 in waterways remain poorly understood. Using long-term streamwater monitoring data, we analyze urban, urbanizing, and rural watersheds across Austin to assess TiO_2 concentrations and their association with dissolved and suspended loads. Baseflow titanium concentrations show little variation across watersheds as well as within the Onion Creek Watershed, where initial reflective pavement testing has begun. Additionally, titanium, while primarily in the dissolved load in these streams, shows significant differences between total (unfiltered) and dissolved (filtered) concentrations, indicating that particulate contributions are significant. This partitioning is important because dissolved and sediment-sorbed metals have different exposure pathways and timelines. Dissolved titanium may travel farther downstream, increasing its exposure radius, while sediment-sorbed titanium can accumulate in benthic environments, posing greater risks to bottom-feeding organisms and introducing new exposure pathways. Additionally, this comparison indicates that environmental assessments based on traditional analysis methods (filtered samples alone) may underestimate the environmental burden from titanium. These findings will help evaluate the impact of climate resilience measures on ecosystem health in an urban setting.

Yale, Vivian., Pinzon, David Bahamon., Banner, Jay., Rempe, Daniella., Hunt, Brian

"Spatial Geochemical Variability in the Middle Trinity Aquifer in a Water Sensitive Region of Central Texas"

Booth # 24

The Hill Country of central Texas is a rapidly growing area that is prone to drought and flood weather extremes. Residents of northern Hays County in central Texas primarily supply their water from the Middle Trinity Aquifer, which also feeds local springs. The increased demand for water resources due to population growth, combined with limited aquifer recharge from sustained droughts, makes local groundwater resources particularly vulnerable. Geochemical analysis offers valuable insights into water quality, residence times, recharge mechanisms, and hydrostratigraphic source areas, which can aid water management strategies. In this study, water samples were collected from 29 sites and subsequently analyzed for major and trace ions. Results support the existence of a previously hypothesized groundwater divide within the Middle

Trinity Aquifer. This divide separates water with a Ca-Mg-HCO3 composition flowing northwest from water with a Ca-Mg-SO4 composition flowing southeast. To the northwest, the Middle Trinity Aquifer is exposed at the surface, allowing direct recharge and shorter residence times. Southeast of the divide, the aquifer is confined by the Upper Trinity Aquifer and is exposed to evaporite deposits, leading to indirect recharge, longer residence times, and high sulfate concentrations. Differences in residence time, chemical composition and salinity are interpreted as the result of spatial variations in hydrostratigraphy. Geochemical analysis of the Middle Trinity Aquifer is important for defining key hydrologic processes and boundaries, which can inform sustainable policies that protect recharge zones and groundwater from the effects of drought and pumping.

Rasmussen, Berit Hudson., Rempe, Daniella., Dralle, David., Hahm, W. Jesse

"Reduced deep root water uptake enhances baseflow following wildfire"

Booth #A-25

Predicting how streamflow responds to vegetation loss from wildfire or drought mortality is especially challenging in mountain watersheds where deeply rooted trees access moisture stored in weathered bedrock. We show that, following fire- and drought-driven mortality in the southern Sierra Nevada, deep vadose zone moisture shifted from (pre-mortality) supporting evapotranspiration to (post-mortality) sustaining slow drainage throughout the dry summer months. Although this drainage flux represents only 10% of pre-mortality evapotranspiration, it now supports dry season baseflow that was previously absent. Seasonal refilling of the reduced vadose zone deficit following fire facilitates groundwater accumulation during the wet season. Conversely, an adjacent forested control site with active root uptake displays greater summer moisture depletion, lower water tables, and reduced summer baseflow relative to the burned site. These findings underscore the critical role of deep moisture dynamics in shaping hydrologic responses to vegetation change.

Marine Geosciences (9 Participants)

Mackin, Caroline., Lowery, Christopher., Borrelli, Chiara., Trendall, Aiden

"Using Laser Grain Size Analysis and SEM imaging to Investigate Changes in Surface Carbonate Producers in the Southeastern Atlantic across the Eocene-Oligocene Transition"

Booth #A-29

Pelagic carbonate production by open-ocean organisms such as planktic foraminifera and calcareous nannoplankton plays a pivotal role in the global carbon cycle, accounting for about half of annual carbonate production. Changes in pelagic

calcifier populations can significantly alter carbonate flux and deep-sea sediment composition. Traditional methods for studying carbonate production and burial, such as CaCO3 weight percentage and carbonate mass accumulation rates, cannot distinguish the relative contributions of different plankton groups to deep-sea sedimentation. While sieving can help separate size fractions, it is time-consuming and lacks finer resolution. Given that deep-sea carbonate sediments are almost entirely biogenic, fractioning them by size offers a means to approximate the relative contributions of different calcifiers. Here, we present results from a method aimed at reconstructing the role of plankton groups in pelagic carbonate production using laser grain size analysis, which allows rapid, detailed quantification of both coarse (>20 μm, largely planktic foraminifera) and fine (<20 μm, largely calcareous nannoplankton) carbonate fractions, as well as trends within those fractions. We applied this method to samples spanning the Eocene–Oligocene Transition (33.7–34.5 Ma) from Ocean Drilling Program Site 1265 (Walvis Ridge, SE Atlantic, 3083 m water depth). Calcareous nannoplankton dominated throughout the interval, comprising ~80–90% of the carbonate fraction. Foraminifera remained minor (<10%), with small, medium, and large size classes contributing modestly but variably. A peak in foraminiferal abundance occurs in the late Eocene, followed by a decline in the early Oligocene. SEM imaging was used to confirm our findings and assess preservation. Despite high and relatively constant carbonate concentrations, SEM images reveal extensive foraminiferal damage, with large, dissolution-resistant species like Globigerinatheka dominating the late Eocene. An increase in planktic foraminifera in Oligocene samples, especially small specimens, indicates improved preservation, consistent with trends at other South Atlantic sites. These findings demonstrate that laser grain size analysis, supported by SEM imaging, can quantify subtle changes in foraminiferal dissolution even in intervals with constant carbonate concentrations, providing more nuanced insights than bulk %carbonate or qualitative preservation estimates alone.

Patwa, Hessa., Malkowski, Matthew., Sickmann, Zachary., Visser, Jason

"Tracking Rare Earth Element Concentrations in San Francisco Bay Depositional Environments"

Booth #A-30

Rare Earth Elements (REEs) are essential for many technologies, such as smartphones, batteries, superconductors, and wind turbines. As demand for REEs increases, recognizing the processes that concentrate REEs in sedimentary deposits is vital in identifying potential sources, especially in accessible coastal zones. Light REE-bearing minerals, such as monazite, and heavy REE-bearing minerals, such as xenotime and zircon, contain many of these crucial REEs. Beaches and tidal ebb-deltas may produce placers, where heavy REEs accumulate due to hydrodynamic fractionation and

by wave and tidal action winnowing lighter particles. To better understand how depositional environments and surface processes affect REE distribution, we combine new and existing geochemical analyses of sediment across regions of the San Francisco (SF) Bay and outer coast. The dataset includes grab samples, dredges, and piston cores of SF Bay area beaches, ebb and flood delta deposits, and offshore marine samples of sand and silt. New samples were powdered and pressed into homogeneous discs and analyzed by wavelength dispersive X-ray fluorescence (WD-XRF) spectrometry to determine the concentration of major and trace elements, including select REEs. We evaluated REE distributions as total REE (REEt) concentration, which is the sum of concentrations of select REEs, and as chondrite-normalized Lanthanum to Ytterbium (La/Yb) ratios, which quantifies the relative fractionation between light and heavy REEs. Bulk sediment REEt concentrations were highest in the ebb delta, with an average of 142.7 ppm and lowest in the beaches, with an average of 45.2 ppm. The estuarine region had an average REEt concentration of 90.4, which is between that of the ebb delta and beaches. The lowest La/Yb ratio was found in a beach environment (Stinson Beach: 1.6), indicating a greater presence of xenotime and zircon, whereas the highest ratio was found in an ebb delta environment (Outer Coast: 9.6). We found that zirconium (Zr) is strongly correlated with REEt (linear fit R^2=0.894), demonstrating that Zr, which is most abundant in zircon, may be a good proxy for concentration.

Amendola, Jonathan., Sherman, Dallas., Gulick, Sean., Goff, John., Jaeger, John., Durr, Rachael., TERMINUS Expedition Team

"Subglacial Erosion Rates Calculated from Proglacial Sediments of a Marine

Terminating Glacier in West Greenland"

Booth #A-31

Marine terminating glaciers deliver an enormous quantity of sediment to the global ocean, but interactions between glaciers and the sediment they create and export remain understudied. As part of the TERMINUS project to investigate causes of tidewater glacier stability, we conducted a geophysical and sedimentological survey of two glacier termini, Kangerlussuup Sermia (KAS) and Kangerluarsuup Sermia (KSS), located in central west Greenland. KAS has remained relatively stable over several decades, whereas KSS has retreated >1.5 km from its 1980s position. We hypothesize that the different volumes of sediment eroded by these systems may be responsible for their divergent behavior. The July-August 2024 research cruise, conducted aboard the R/V Celtic Explorer, utilized shipboard chirp seismic and multibeam bathymetry systems, in addition to a high resolution multichannel seismic reflection (MCS) system with a GI gun source and 350 m streamer length featuring denser near channel spacing. Using the chirp and MCS reflection data, we identified seismic facies that we interpret to represent paleomoraines, ice-proximal, ice-distal, and periglacial sediment deposits that

allow for reconstructions of past termini positions. We find in both systems a prominent moraine assumed to be formed during the Little Ice Age (LIA) outboard of an overdeepened basin. In KAS, MCS and chirp data reveal an outer basin infilled with complex sediment packages recording retreat and advance facies overtopped by an extensive submarine drainage system feeding a substantial submarine delta. In KSS, the LIA to 1980s retreat facies are relatively limited, and sedimentation since the 1980s is limited to low amplitude cyclic steps on top of the partially exposed morainal complex. We use the internal structure of the submarine delta deposits to determine areal extent, formation processes, and relative age. Using these data, we derive post-LIA sediment volumes and use these to estimate preliminary basin-scale erosion rates for both systems. We intend to use these basin sediment volumes to establish post-LIA sedimentation and erosion rates for KAS and KSS to better understand the factors that drive subglacial erosion and proglacial sedimentation.

Greiner, Kylie., Gulick, Sean., Shuck, Brandon

"Legacy Marine Seismic Data Reprocessing and Interpretations within the Accretionary Prism in the Southern Portion of the Cascadia Subduction Zone"

Booth #A-32

We are reprocessing legacy marine seismic data from the 1994 Mendocino Triple Junction Seismic Experiment (MTJSE). This is the most recent dataset for the southernmost portion of the Cascadia Subduction Zone (CSZ) and for the Mendocino Triple Junction (MTJ). We are concerned with reprocessing these data because there is a gap in the data from the recent CASIE21 (Cascadia Seismic Imaging Experiment 2021) that collected new data for most of the CSZ except for northern California. This gap needs to be filled in order for assessments of hazards as well as the generation of velocity, slab, deformation, etc. models to be created. Constraining hazards is important for this margin because there is uncertainty about when the next megathrust event will be and if it will be similar to the Mw9> and the transpacific tsunami that occurred in 1700.

The preliminary reprocessed images from four dip lines across the CSZ show a change in vergence within the outer wedge of the accretionary prism from north to south, MTJ14, MTJ8, MTJ12, and MTJ6 respectively. MTJ14 shows a dominant landward vergence. MTJ 8 and MTJ12 show a dominant seaward vergence with a possible transition to landward vergence as MTJ8 moves eastward, whereas MTJ12 stops before this transition. MTJ6 lies close to the MTJ, so it shows a mixed vergence in the outer wedge due to the complex interplay from the CSZ and MTJ. The downgoing Gorda plate and the décollement are images fairly well throughout the lines.

We are also reprocessing six additional lines that will be helpful for further constraining the MTJ and the accretionary prism because the strike lines will be helpful to further constrain the accretionary prism. In addition, we will be using newly released

bathymetry data for the region to look for fault scarps and tie into with our final interpretations.

Margoshes, Jacob., Covault, Jacob., Sweet, Michael

"Debris-flow-driven Avulsion of Submarine Channels, Late Pleistocene Joshua System"

Booth #A-33

In rivers, avulsions, which are the abrupt abandonment of an existing channel course in favor of a new one, are extensively documented, and their triggers have been constrained across various settings. However, the processes of submarine channel avulsions have yet to be directly observed. We use three-dimensional seismic-reflection data (with a dominant frequency range of 30-40 Hz) from the eastern Gulf of Mexico to document the stratigraphy of an avulsion in the Joshua submarine channel system and to interpret its trigger. Just prior to avulsion, the channel fill comprises low-amplitude, mottled seismic reflections, rather than the high-amplitude, V-shaped reflections characteristic of channel-axis deposits found elsewhere in the system. In plan view, this channel fill shows individual blocks (exceeding 200 meters in diameter) surrounded by a low-amplitude matrix. We interpret this unique reflection character as a debris-flow deposit that plugged the active channel. Following this blockage, the next channel in the sequence avulsed to follow a new course on the seafloor; subsequent sinuous channels in the new belt exhibit systematic meandering. As debris flows are common in deepwater settings, this avulsion mechanism likely occurs across a variety of basins, especially in environments with high sedimentation rates that promote mass wasting and long run-out gravity flows.

Paz, Mia., Shank, E. M., Lowery, Christopher

"Foundational Compilation of Foraminifera Biodiversity in Corpus Christi Bay"

Booth #A-34

Modern foraminifera are often used as proxies for temperature, salinity, sedimentation rates, and pollution. Around the Gulf of Mexico, efforts have been made to compile an updated catalogue of data on the different species and their abundance in the bays, which can be used for future research in tracking environmental changes. The general problem is that there is a lack of data and information about benthic foraminiferal populations. This is particularly true for Corpus Christi Bay, along the Texas Coastal Bend. Although some work has been published on benthic foraminifera from Nueces Bay (at the top of Corpus Christi Bay) and from a handful of sites on the bay side of Mustang Island (at the bottom of Corpus Christi Bay), there has been no published work on living benthic foraminifera populations through most of the bay. Here, we create the first map

of foraminiferal biodiversity throughout Corpus Christi Bay. This can then be used as a baseline for future samples to track benthic biodiversity changes due to anthropogenic effects. Across Corpus Christi Bay, 19 samples were taken at various locations to create an even spread of samples and data. Each sample was taken via grab sampling in August of 2025 and contains 50 milliliters of mud soaked in a Rose Bengal solution to stain the living and recently living specimens, which are currently being picked out under a microscope for population analysis. We expect results to show anthropogenic effects negatively impacting biodiversity in the foraminifera populations in Corpus Christi Bay. Therefore, by having a basis of foraminifera in this location to track changes, action can be taken to protect and limit the effects of human activity and help solidify limitations on emissions and possible implementation of protected areas. With the influx of human effects, such as dredging, commercial boat traffic, and pollution, it is more important than ever to focus on and analyze foraminifera. Since foraminifera are great proxies for environmental changes, they can be used as identifiers for changes in water quality, which can then be used to understand how humans are impacting the water in our bays.

Guzmán, Cassandra., Mohrig, David., Sylvester, Zoltán

"Reworking and Filling of an Ephemeral Barrier Island Inlet Formed by Hurricane Beryl, 2024, Texas"

Booth #A-35

Inlets cutting barrier islands, natural or man-made, can alter the impact hurricanes have on marshland, estuaries, shipping ports, fishing industry, and homes, yet their formation is incompletely understood. On July 8th, 2024, category one Hurricane Beryl made landfall at East Matagorda Bay creating a new inlet on the Matagorda barrier peninsula, 2.2km southwest of the man-made Mitchell's Cut, and 2.3km northeast of a closed natural inlet, Brown Cedar Cut. Storm surge from the hurricane created a large overwash fan crossing the entire peninsula and depositing sand in the bay. After landfall, changing wind direction drove a seaward directed surge with the resulting outwash reworking the fan, eroding some of the newly deposited sediments, and further widened the inlet. Following passage of the storm, the newly formed inlet changed in size and shape monthly, initially pointing towards the channel remaining open, but by December 2024 the inlet was filled almost entirely with sediment, and as of January 2026, there has been minimal change in its shape. This study focuses on determining the dominant processes that kept the ephemeral inlet open and the processes that eventually closed it. Preliminary data show storm surges and high-water levels during the 2024 hurricane season kept the inlet open, but sediment transported via longshore currents and wave-action closed it once hurricane season was over. The creation of this ephemeral

inlet and its sensitivity to day-to-day processes may alter how future storms and hurricanes impact the barrier island and estuary of East Matagorda Bay.

Gutiérrez, Juan., Sweet, Michael., Covault, Jacob., Sylvester, Zoltán., Margoshes, Jacob

"Submarine canyon morphology records river dynamics and seascape evolution,

Pleistocene Mississippi canyons"

Booth #A-36

Utilizing time- and depth-migrated 3D seismic-reflection data, we mapped the basal unconformities of ten Pleistocene submarine canyons on the present-day Louisiana shelf. Excluding the Bryant and modern-day Mississippi canyon, these features have not previously been mapped or described in detail. Despite significant variability in the overall canyon shape, with incision depths of 0.2–1.1 km, widths of 6–12 km, and upstream incision lengths of 40–100 km from the shelf edge, the basal thalweg widths remain consistent, ranging between 200 m and 250 m. This suggests a similar sediment input for all ten systems: the paleo-Mississippi River. Consequently, we interpret these canyons to be a record of Mississippi River migration across the Pleistocene coastal plain.

We measured canyon morphologies (i.e., cross-sectional areas, incision depths, and thalweg longitudinal profiles) to interpret the spectrum of canyon maturity and longevity within this succession, assuming a relatively constant sediment input from the Mississippi River. Radiocarbon ages indicate that the modern Mississippi Canyon initiated between 50,000 and 30,000 BP, remaining active until 20,000 BP. This age control provides a benchmark for assessing the longevity of ancestral Mississippi canyons based on morphology. Deep, wide incisions, like for the modern Mississippi Canyon, indicate longer-lived systems of sufficient duration to develop a mature axial channel belt. Conversely, shallower and narrower incisions represent shorter-lived systems that were abandoned before a wider channel belt could evolve.

Bai, Wilson., Martindale, Rowan., Sylvester, Zoltan., Trower, Elizabeth., Bodin, Stéphane., Kabiri, Lahcen

"Determining Carbonate Chemistry Changes across the Toarcian Oceanic Anoxic Event

using Ooid Sizes and Machine Learning"

Booth #A-37

The Toarcian Oceanic Anoxic Event (TOAE) is a global climate perturbation in the Early Jurassic Period. The environment changed rapidly due to the Karoo-Ferrar large igneous province eruptions, which released abundant greenhouse gases, such as CO2,

into the atmosphere, causing global temperature increases. It has also been speculated that ocean acidification occurred during the TOAE; however, current data are insufficient for a definitive conclusion. Reconstructing ocean acidification in deep time is difficult due to the corrosive nature of acidification.

The scientific community has primarily tried to identify paleo-acidification using dissolution horizons (such as carbonate gaps) or boron and strontium stable isotopes. Here, we present another proxy for ancient carbonate chemistry: using ooid size as a proxy for acidification across the TOAE. Ooids are small (~2 mm) spherical carbonate grains made via carbonate precipitation around a central nucleus, which can be a skeletal fragment, grain, or other material. The carbonate saturation state (Ω) is proportional to ooid size, therefore we can use ooid grain size to model ancient Ω. Oolites from the High Atlas Mountains in Morocco were chosen because several field sites preserve high-resolution records of ooid grainstones from before, during, and after the TOAE interval.

Thin sections of oolites from Morocco were photographed using a Zeiss Imager M2m petrographic light microscope. These microphotographs were fed into 'segmenteverygrain', a Python package which outlined ooids using a machine learning model that was trained to segment a variety of grain types. We trained an ooid-specific machine learning model, using a dataset of manually segmented and quality controlled ooid images. After segmenting the ooids, the program measured minor axes of the grains to prepare for Ω calculations. When plotted against stratigraphic height, ooid minor axis length generally decreased with the onset of the TOAE and showed slow recovery towards pre-TOAE ooid sizes. This project demonstrates the use of a new protocol for measuring and converting ooid diameters to ocean acidification indicators. Carbonate saturation state is then calculated from ooid sizes via the Oomega Solver protocol. Next steps include calculating pH using PHREEQC and statistical analysis.

Quantifying carbonate chemistry in ancient oceans would allow us to better understand the impact of past ocean acidification events. These records will help us predict how modern species may respond to current acidification conditions. The protocol for quantifying acidification in deep time is not only novel but can be highly automated.

Geobiology (4 Participants)

Sennello, Joseph Rocco

"Morphometric Analysis of Ontogeny in Cranial and Pectoral Elements of North American Metoposaurs"

Booth #A-48

The phylogenetic relationships within the Late Triassic amphibian family Metoposauridae remain unresolved, in part due to substantial ontogenetic variation in cranial morphology. Building on previous morphometric work on Buettnererpeton bakeri,

this study expands ontogenetic analysis to additional metoposaurid taxa from the American Southwest, including Apachesaurus gregorii and Koskinonodon perfectus. Using landmark-based geometric morphometrics, this project investigates cranial growth patterns within and between species to evaluate whether shared developmental trajectories can inform metoposaurid phylogeny.

Dorsal-view photographs of museum specimens were collected and analyzed using ImageJ and MorphoJ, with landmarks placed at reproducible sutural intersections and key cranial features. Principal Component Analysis was used to quantify major axes of shape variation and compare ontogenetic trends. Preliminary results from Buettnererpeton bakeri indicate distinct changes in skull proportions through growth, particularly in anterior–posterior elongation and lateral expansion. These results highlight the importance of ontogenetic context in metoposaurid systematics and suggest that developmental patterns may clarify evolutionary relationshipswithin Metoposauridae.

Canamar, Janet

"A Fossil Stem-Galliform (Aves, Paraortygidae) from the Late Oligocene Armissan Quarry of France"

Booth #A-49

Taoperdix pessieti is a rare stem-galliform (landfowl) referred to the family Paraortygidae and known from Oligocene limestone deposits of France. Despite the genus being cited in the literature on Cenozoic birds, the type species *T. pessieti* has not been comprehensively described or critically re-evaluated. Here, we examine two attributed *T. pessieti* skeletons housed at the Carnegie Museum of Natural History (CM 4023 and CM 4459), originating from the Late Oligocene Armissan Quarry, to assess their osteological morphology in comparison with other referred *Taoperdix* material and closely related Paleogene galliform birds. These skeletons have not been previously described and provide new anatomical data relevant to the Paraortygidae. Through comparative anatomical analysis, this study aims to clarify morphological characters pertinent to the taxonomic placement of *T. pessieti* and to reassess its systematic position within early galliform evolution.

Canamar, Janet; Fuentes, Javier-Jose; Tykoski, Ronald

"Quantitative Analysis of Elasmobranchii teeth from the Lewisville Formation (Woodbine group) of North Texas"

Booth #A-50

Extinct Elasmobranchii (sharks, rays, skates) are described by their isolated teeth, due to their abundance in marine fossil records. The Western Interior Seaway supported diverse marine life, including Elasmobranchs. Three outcrops located in the Dallas-Fort

Worth area in Texas expose the Lewisville Formation, an Upper Cenomanian (101.5-93.9 Ma) unit, a part of the Woodbine Group known for preserving aquatic and terrestrial ecosystems. An approximate number of elasmobranch teeth were collected from each locality. The teeth collected explore unidentified dental characteristics that have yet to be figured, requiring a statistical analysis of the features. Additionally, a re-evaluation of reported elasmobranchs from the Woodbine group has not been assessed. A revision is essential to document the newly acquired evidence of elasmobranchs present in Lewisville. To conduct this examination, high-resolution pictures of each tooth were scanned into an analytical software program (ImageJ) to collect measurements and placed in a principal component analysis (PCA). A descriptive analysis was conducted to properly evaluate each elasmobranch species identified. The quantitative data present a systematic evaluation of the diversification of elasmobranch species from the Lewisville Formation.

Foster, Brooklyn; Kadam, Ira; Shero, Riley

"Vertebrate Fossils from a Cave Site in the Lady Bird Johnson Wildflower Center Suggest a Record of Recent Ecological Change in Austin"

Booth #A-51

Cave fossil assemblages provide important records of past ecological communities. For locations like the Austin metropolitan area, with limited fossil records, studying cave assemblages and identifying the represented animals is key to understanding past local animal life. Here we identified two lower canines and an upper molar recovered from a cave at the Lady Bird Johnson Wildflower Center, using comparative morphological analysis and paired t-testing of dimensional measurements against extant reference collections. Both analyses identified the larger canine as an ursid (i.e., a member of the bear family, Ursidae), likely Ursus americanus, and the smaller canine as a canid (i.e., a member of the dog family, Canidae), either Canis latrans or Canis familiaris. Diagnostic morphology indicated that the molar belongs to a member of Caprinae, which includes sheep and goats. Native caprines are poorly suited for the local habitat, so the molar is likely from a domesticated species. Radiometric dating was not performed, and specimens cannot be assumed to be the same geologic age. However, domesticated caprines are unknown in North America prior to 1559 CE. Relevant ursids and canids have been in North America for ~750,000 years. Black bears existed in the area until ~1900 CE. It is possible that the identified animals existed contemporaneously in the Austin area as a Holocene vertebrate community including native and introduced species. This discovery demonstrates that small, urban cave sites can preserve informative records of recent ecological change and serve as paleontological resources in areas with limited fossil records.

Planetary Sciences (10 Paricipants)

Alfred, Soraya., Hesse, Marc., Gulick, Sean., McCall, Naoma., Rae, Auriol., Tikoo, Sonia

"66 Million Years of Sustained Hydrothermal Convection at Chicxulub Crater"

Booth #A-38

Impact craters have been under increasing investigation as viable sites for microbial evolution due to their potential to facilitate the generation of prebiotic chemistry. The Chicxulub impact structure shows evidence of an extant microbial community and hydrothermal alteration. The Chicxulub impact event led to the end-Cretaceous mass extinction, and its post impact hydrothermal system has been suggested as a catalyst for the rapid recovery of life shortly thereafter. Consequently, the system has been modelled to determine its lifetime and its link to endolithic colonization. Adopting a different approach, we have utilized modern day properties, from drilling operations, in tandem with previous studies and data to create a new model for hydrothermal convection. Model geometry was informed by seismic surveys while properties were prescribed based on core sample measurements and hydrocode simulations. Results suggest that fluid circulation is currently active within the crater, even though the initial heat has dissipated. Pre-impact sediments have been relocated multiple kilometers beneath their origin and increased in permeability. In contrast, adjacent granitic basement was uplifted up to 10km and experienced shock metamorphism, thereby also increasing permeability. These lithologic units provide ideal pathways to transport hydrothermal fluids and overlying, low permeability melt rock and suevite limit fluid escape. Assisting in the system's longevity is the irregular lateral temperature distribution, elevated in the crater's central region, indicating that impacts can generate lasting thermal anomalies that can ultimately support microbial communities feeding off hydrothermal systems for an indefinite amount of time.

Xiong, Timothy., Flemings, Peter., Hesse, Marc., Ketcham, Richard., Tisato, Nicola., McCarthy, Christine., Zaman, Maheenuz

"Quantifying Compaction Viscosity During Compaction of Partially Molten Polycrystalline Ice: Instrument Development and Numerical Modelling"

Booth #A-39

The compaction viscosity of partially molten polycrystalline ice governs its compaction and affects mass and heat transport. Although it is a crucial physical property and parameter in modelling glacier and planetary icy shell dynamics, the compaction viscosity is often back-calculated or sensitivity-studied due to a lack of both experimental

measurements and understanding of pore-scale mechanisms. To bridge this gap, we developed an X-ray transparent, cryogenic, triaxial loading device that allows for micro-CT imaging of geomaterials, including ice, during compaction. The device accommodates cylindrical samples with a diameter of 12.7 mm and a height of up to 55 mm. It can apply confining pressures of up to 25 MPa and axial stress of up to 33 MPa with temperature control (down to -25°C) and pore fluid flow control capabilities. We present design details and demonstrate the ability to measure permeability and Young's modulus of a clay sample. We plan to first apply isotropic loading on synthetic partially molten saline ice specimens while measuring pore pressure and deformation. To facilitate interpretation of experimental data, we have also developed 2D cylindrical, coupled, finite difference models for both poroelastic (Biot) and poroviscous (Darcy-Stokes) materials that predict different pore pressure response and porosity evolution.

Carrington, Morgan., Goudge, Tim., Johnson, Joel P.L., Hopkins, Dejah., Bonilla, Roxell

"Amphitheater-headed canyons on Earth and Mars: Insights from Geomorphic Modelling and Drone-based Remote Sensing"

Booth #A-40

Amphitheater-headed canyons are morphologically distinct valleys, characterized by stubby, curved canyon heads, near-constant valley width from source to outlet, and large-scale topographic relief. In contrast to other incised martian valleys, such as more typical 'valley networks', amphitheater-headed canyons are thought to have formed later in Mars history when surface water activity was more sparse, episodic, and/or spatially-focused. This suggestion, in addition to observations of morphologically similar canyons on Earth, has motivated deeper investigations into the hydrologic processes responsible for their formation. Groundwater seepage and overland flow have been proposed as formative processes that contribute to amphitheater-headed canyon formation, but their relative roles remain highly debated on both planets.

Here, we present work from two projects that utilize different approaches to constrain contributions from the proposed formation mechanisms. In the first project we apply a simple knickpoint retreat model that is driven by upstream surface drainage area, a proxy we use to estimate discharge from surface runoff, to 25 amphitheater-headed canyon systems on Earth and 34 systems on Mars. Our results reveal that the model is able to reliably predict canyon head locations on both Earth and Mars; however, model predictions on Mars are a factor of ~2 more accurate. Additionally, we find that the non-linear dependence on drainage area differs between Earth and Mars, with martian amphitheater-headed canyons requiring a larger surface drainage area to achieve the same retreat rate as terrestrial canyons. Combined, our results suggest that runoff production on Mars was inefficient compared to Earth and that additional contributions from other

formative processes, such as groundwater seepage, may be necessary for martian canyons.

The second project focuses on the unique and enigmatic morphologies of amphitheater-headed canyons on Earth, where we are seeking to characterize the 3D viewing perspective in order to determine how the proposed formation processes can be expressed. As we continue to develop this project, we aim to determine if and how the 2D planform morphology is able to capture the processes expressed in the 3D – a distinction that may also provide insight into the formation mechanisms responsible for canyon formation on Mars.

Kinney, Adam., Johnson, Joel., Abdallah Zaki

"Topographic Analysis of Martian Canyon Morphology in Ius Chasma Utilizing Analog Formations in Haleakalā, Hawai'i"

Booth #A-41

The environments of Haleakalā, Hawai'i and the Ius Chasma region of Mars show observational similarities in basaltic canyon structure. Further analysis of these comparable landscapes could provide clues about the similarities in Martian erosional processes. On Mars, these structures are predicted to have formed as a result of either groundwater sapping or overland flow. The valleys of Haleakalā are developed through mass wasting and runoff, and will be used as a reference for the forms this type of erosional environment supports. This study critically evaluates the hypothesis that the amphitheater-headed canyons in Ius Chasma are the product of overland flow and mass wasting. If topographic analysis using remote sensing data reveals that these valleys have similar slope, curvature, and roughness, it would support that the Martian valleys similarly evolved resulting from surface water flow. The theory that the valleys' formation was under the influence of groundwater sapping would be more likely if the slopes have incongruent morphology, especially if the Martian valleys have steeper slopes.

Stephenson, Milo., Grima, Cyril., Gulick, Sean

"Investigation of Radar Bright Lava Flows in Elysium Planitia, Mars"

Booth #A-42

Between 2012 and 2015, the Mars Advanced Radar for Subsurface and Ionosphere Sounding (MARSIS) collected profiles in the 4 MHz band containing anomalously bright subsurface reflections beneath the Martian South Polar Layered Deposits (SPLD), which were hypothesized to be evidence of subglacial liquid water. However, previous work applying a forward approach using MARSIS surface reflectivity measurements demonstrated that volcanic terrains could produce a basal reflection of

similar magnitude to the one observed beneath the Martian SPLD if these terrains were covered by ice. We extend this work by investigating the non-uniform distribution of MARSIS surface reflectivity in the previously identified lava flow unit CP19 within the Cerberus Plains. We identified two distinct regions within this lava flow unit: a radar-bright region with patches of exceptionally bright radar returns analogues to the SPLD basal detection and a radar-dark region which lacks them and possesses a lower average surface reflectivity. The distinction between these two regions is further demarcated by contrasting surface temperatures observed in daytime infrared images by the Mars Odyssey Thermal Emission Imaging System (THEMIS) and differences in surface texture observed in images acquired by the Mars Reconnaissance Orbiter's Context Camera (CTX) instrument. We used published thickness estimates of lava flows from Mars SHAllow RADar sounder (SHARAD) to show that the radar-dark region has a higher average thickness than the radar-bright region. Additionally, we used these thickness estimates to test whether the difference in average surface reflectivity is attributable to constructive interference from fraction of a wavelength bed thickness, or whether there are contributions from surface roughness differences or geologic properties. The underlying differences between these two regions may provide insight into why only some volcanic terrains exhibit such a strong signal.

Prakash, Medha., Gulick, Sean., Grima, Cyril., Milliken, Ralph., Lambert, Philippe., Goudge, Tim., Robertson, Kevin

"Impact-induced hydrothermal alteration at Rochechouart and Chicxulub in the eyes of reflectance spectroscopy"

Booth #A-43

Impact-induced hydrothermal alteration is potentially a crucial process for the origins of and rebound of life after mass extinction. Understanding the spatial and temporal evolution of impact-induced hydrothermal systems is imperative for constraining the most probable environments in the search for extraterrestrial life. Factors that may influence this evolution include the energy upon impact, target mineralogy and composition, porosity of shocked rock, and fluid chemistry. These facets can be directly understood by examining the mineralogy of hydrothermally altered impact products, as mineral precipitation can be ascribed to specific thermodynamic and chemical conditions. A diverse array of hydrothermally altered impactites are found at the Rochechouart Impact Structure. The Rochechouart Impact Structure is a 23 km diameter structure centered in the Charente Department of France. The crystalline target lithology is comprised of granodiorite and gneisses with felsic and more mafic compositions. This heterogeneous target likely led to the large variety of melt-rocks and breccias seen in the 540 m of cores drilled today. Here, we use Visible-Near Infrared (VNIR) Spectroscopy, a remote sensing method sensitive to hydrothermal alteration products

(e.g. clays and oxides), to explore the variations in hydrothermal alteration based on target heterogeneity and impactite type throughout the basin. Initial examinations of the VNIR data show distinct signatures for different breccia, melt rock, and altered basement lithologies, while being relatively insensitive to clast type, size and density. This work would be the first major characterization of the spatial distribution of hydrothermal alteration in Rochechouart and offers ground-truth to spectra of impactites obtained from remote sensing of planetary surfaces. This work also advanced local knowledge of the impact site, through participating in outreach events such as Asteroid Day. Future work includes detailed analyses of specific impactites using X-ray diffraction (XRD) and micro-Fourier transform infrared spectroscopy (Micro-FTIR), to increase sensitivity to alteration minerals that are not salient in VNIR, such as zeolites, sulfides, and opal.

Neary, John., Hesse, Marc

"MODELING FLUID LIMITED PROPAGATION OF SERPENTINIZATION FRONTS IN ULTRAMAFIC ROCKS"

Booth #A-44

Hydrogen formed by the oxidation of ferrous iron is a fuel for life in the subsurface. Ancient mafic and ultramafic rock bodies undergo active hydration reactions on Earth, producing streams of H 2 rich fluids. Reaction rates derived from lab and field measurements of gas fluxes predict reaction exhaustion timescales that are short compared to the age of the rock bodies, and cores reveal a zone of increasing hydrous alteration on the tops of mafic and ultramafic rock bodies. The apparent paradox of long reaction life in fast reacting systems and the observation of gradational hydration zones leads us to hypothesize that the water supply is the dominant control on the progress of hydration reactions in ultramafic systems. To model the supply of water to the reaction zone, we combine simplified models of permeability and reaction front pressure. In the 1D case, the propagation of the front increases the distance from the hydraulic head boundary to the reaction front, thus decreasing the pressure gradient. Using a numerical model to analyze the 2D case, we also find that the presence of fractures and their geometry exert strong controls on reaction time scales. As expected, the reactions slow dramatically over time. We attribute this to the increasing thickness of low permeability reacted rock around the fracture through which water must flow.

Jackson, Heidi T., Young, Duncan A., Chan, Kristian., Blankenship, Donald

"Utilizing Delay-Doppler Processing techniques to discern firn structure over Devon Ice Cap"

Booth #A-45

Understanding firn structure is critical in interpreting ice-penetrating radar (IPR) returns and identifying near-surface scattering artifacts at depths within approximately two wavelengths. Radar Statistical Reconnaissance has previously been used to separate and isolate the coherent (P c) and incoherent (P n) components of the radar return, showing that the P c /P n ratio correlates well with firn structure and geographic zones over Devon Ice Cap (DIC) in the Canadian Arctic. DIC has been previously used as a terrestrial analog to understand how radar reflectometry can be utilized to characterize near-surface heterogeneity for REASON at Europa.
We propose an alternative method utilizing Delay Doppler Processing (DDP) to parameterize surface echo strength and infer firn structure, which may expand upon the efficacy of DDP to further constrain scattering and produce more coherent returns in dopplergrams of very high frequency (60 MHz center frequency) IPR data. In our approach, coherent power is derived by extracting the peak return power in each Doppler slice, which is then calibrated using the image method spherical wave reflection to estimate surface reflectivity. To quantify the scattered component, we assume a simple relationship between the return strength and coherent and incoherent components. The total return power is determined by integrating peak-power per return angle within the pulse-limited footprint. Using this methodology, we aim to differentiate firn containing thin ice lenses, firn with thick ice slabs, and fully densified glacier ice layered within firn. This technique further constrains spatial characterization of firn zones and distinguishes scattering within dopplergrams. Future work will extend this technique to distinguish the effects on near-surface scattering due to these heterogeneities from the dielectric contributions of targeted geological landforms.

Bellino, Lucia., Sun, Chenguang

"Sulfur Degassing on Io Constrains Its Volcanic Processes and Redox Evolution"

Booth #A-46

Vigorous volcanic activity on Jupiter's moon, Io, sources widespread surficial sulfur and SO_2 frost [1] and a thin, SO_2-rich atmosphere with an extremely heavy sulfur isotopic composition [2]. Recent models propose that this atmospheric isotopic signature is resultant of significant sulfur depletion from the interior of Io [2, 3]. However, this notion conflicts with the abundant, sulfurous volcanic plains on the Ionian surface [1] and consequently obscures the subsurface magmatic processes, sulfur inventory, and redox evolution of Io. To address this sulfur dichotomy, we first estimate the S_2/SO_2 ratio of global Ionian magmatic emissions by calculating the abundances of sulfur and SO_2 stored in the crustal and atmospheric reservoirs of Io with mapped geologic units [1] and time-integrated loss of atmospheric SO_2 [3, 4]. This yields a globally averaged S_2/SO_2 ratio of ~6 in Ionian magmatic gases, ~1–2 orders of magnitude greater than previous estimates [5, 6]. We assess the redox condition and bulk sulfur of Ionian magmas with Monte Carlo

degassing simulations, conducted with the *Magma and Gas Equilibrium Calculator* [7, 8] and constrained by the revised gaseous S_2/SO_2 ratio and SO_2 flux on Io [3, 9]. Our results indicate that the interior of Io maintains similar redox conditions to the terrestrial upper mantle ($\Delta FMQ \approx 0$) and produces sulfide-saturated primary melts. We suggest that the interior of Io remains sulfur-rich with a near-primordial sulfur isotopic composition.

Jordan, Mercedes., Grima, Cyril., Gulick, Sean., Prakash, Medha., Thornten, Ian

"Extraction and Analysis of Near-Surface Properties from Low-Frequency Lunar Radar"

Booth #A-47

The Moon's surface has long been analyzed using various imaging and spectroscopic techniques; However, these instruments are sensitive only to the upper micrometers to millimeters of the lunar surface, limiting their ability to probe materials at depth. As a result, ground-penetrating techniques such as radar are required to investigate the physical and compositional properties of mare basalts beneath the Moon's global regolith layer. The Lunar Radar Sounder (LRS) instrument was designed to image deep lunar subsurface structure using low-frequency radar (5MHz). By isolating and analyzing the surface echo, this same dataset can be used to probe near-surface (<75 m) physical properties that are inaccessible to optical
techniques. In this work, we use LRS radar surface reflectivity to examine physical heterogeneities within the nearside lunar maria.

We first describe the construction of radar surface reflectivity data products, including key filtering and processing steps. Focusing initially on a restricted region of interest, we observe a correlation between radar power and ilmenite abundance. When the region of interest is expanded to encompass the lunar maria more broadly, however, this relationship breaks down, particularly across Mare Tranquillitatis, the oldest basin in the study area.

This breakdown motivates an investigation of mare age as a controlling variable. Using a piecewise multiple linear regression, we find that radar surface reflectivity varies systematically with basalt emplacement age, indicating that physical evolution processes may play a primary role in controlling radar behavior at regional scales. We propose two porosity-based hypotheses to explain these age-dependent trends, relating variations in radar power to differences in bulk porosity structure within the upper basaltic substrate.

Finally, we discuss the limitations of our previous calibration of LRS surface reflectivity. Existing calibration relies on a single-layer model using permittivity measurements estimated by data from the Chang'e-5 lander over Oceanus Procellarum. We outline a future calibration approach using a thin-layer model that incorporates both regolith and basaltic permittivities constrained by Apollo samples and local regolith thickness estimates.

Other: Cryosphere, Seismology, Meteorology, and Rock Physics

Cryosphere (2 Participants)

Kerr, Megan; Young, Duncan; Yan, Shuai; Pierce, Christopher

"Current Antarctic Geothermal Heat Flow Models Do Not Capture South Pole Basin Heterogeneity"

Booth #A-54

Accurate estimates of geothermal heat flow (GHF) are critical for predicting basal melting and identifying stable sites for ancient ice, yet GHF remains one of the least constrained boundary conditions for the Antarctic Ice Sheet. Here we evaluate seven published Antarctic GHF models against independent radar observations of subglacial water from the NSF Center for Oldest Ice Exploration in the South Pole Basin (SPB), a geologically complex region on the southern flank of Dome A, East Antarctica. We also simulate optimal GHF fields via a three-parameter Markov chain Monte Carlo algorithm to constrain the spatial variability required by the wet/dry bed conditions. We show that the SPB cannot be characterized using existing GHF maps; instead, constraining basal thermal state in this region will require higher-resolution geophysical data, methods sensitive to shallow crustal heterogeneity, and the integration of radar-based indicators directly into model frameworks.

Reeves, Hunter; Blankenship, Don; Yan, Shuai; Young, Duncan; Grima, Cyril; Cavitte, Marie; Koutnik, Michelle; Andersen, Conor

"Using Radar Observations and Ice Flow Modeling to Investigate Constitutive Properties of Accreted Ice from Subglacial Lake Vostok, East Antarctica"

Booth #A-55

Lake Vostok, Earth's largest subglacial lake, has been a target of study for the past few decades because of its size and unique characteristics. Airborne ice-penetrating radar surveys flown by UTIG during the 2000-01 field season in the Lake Vostok region show evidence of accreted ice stemming from the lake and being carried over the subglacial mountains on the southeastern coast of the lake along the direction of ice flow. The evidence for accreted ice in the form of a change in radar character from Lake Vostok can be observed between the deepest stratigraphic reflection and the bed. It is expected that poorly constrained thermodynamic processes in the accreted ice result in unknown dielectric contrasts allowing for its upper boundary to be observed in radar above the subglacial mountains. As the accreted ice is transported over the mountainous bed, the ice is subjected to large variations of stress and strain compared to the low stress-strain environment over the lake when the ice was originally accreted. The accreted ice is hundreds of meters thick in some areas and may have a different

constitutive law governing the ice body compared to the roughly three-kilometer-thick stratigraphic ice above. To investigate this, the boundaries of the accreted ice were traced in the radar data and will be used to inform a 2.5-D ice flow model. This model will be used to better confine the stress-strain environment within the stratigraphic ice and of the accreted ice over the jagged bed. We present a new flow line which is parallel to the ice flow direction and a database of uniformly picked accreted ice across Lake Vostok as a set up for modeling. The contrasting constitutive laws will be determined for both the accreted and stratigraphic ice from this study enable a better understanding of the role of more widespread ductile ice deformation associated with accreting basal ice across the Antarctic ice sheet. In addition, these results will provide a potential framework for understanding the flow reorganization of accreting ice systems for other ice-covered ocean worlds of the solar system.

Seismology (1 Participant)

Hezam, Odai., Bakulin, Andrey., Titova, Anna

"Observations of Ambient Seismic Noise on Offshore Telecommunication Fiber using Distributed Acoustic Sensing (DAS)"

Booth #A-52

Applications of Distributed Acoustic Sensing (DAS) have been widely studied in seismic imaging, enabling more cost-effective approaches compared to traditional seismic acquisition. In offshore settings, the industry has typically relied on ocean-bottom instruments and active sources, which are often expensive and have limited spatial and temporal resolution. DAS measurements obtained from telecommunication fiber-optic networks can be highly valuable for passive seismic imaging and monitoring. In this study, we analyze ambient seismic noise recorded along a 65-km cable deployed on the seabed off the coast of Freeport, TX, with 5091 channels spaced 12.79 meters apart, to assess the feasibility of DAS for interferometric applications.

We use raw DAS measurements, recorded as optical phase changes, to compute strain series and convert them to acceleration spectral density. Then, we compare noise spectra against Peterson's New Low and High Noise Models. Compared to active seismic methods, which are source-bandwidth limited at low frequencies, DAS can reliably resolve low frequencies (0.025–2.5 Hz) through long continuous passive recordings. These low-frequency signals are dominated by ocean gravity waves, with pronounced spectral peaks around 0.15 Hz, and spectra that fall consistently within the expected Peterson bounds.

These observations lay the groundwork for passive seismic noise analysis by leveraging existing offshore fiber-optic infrastructure and DAS capabilities. The dense spatial sampling and long temporal coverage provided by DAS support conducting interferometric studies, including the retrieval of coherent seismic signals, dispersion

analysis, and surface-wave inversion. The results demonstrate that these measurements can reliably capture ambient noise suitable for passive seismic imaging.

Meteorology (1 Participant)

Talukdar, Sasanka., Garcia, A. C., Muller, C., Yang, Z. L., Gopalakrishnan, S., Niyogi, D.

"Convective Cold Pools and Hurricane Intensification: A Case Study of Hurricane Helene (2024)"

Booth #A-53

Convective cold pools—dense, cooled air masses generated by rainfall evaporation—are key regulators of atmospheric convection, yet their role in hurricane dynamics remains poorly understood. This study investigates their impact on the intensification of Hurricane Helene (2024) using simulations conducted with a modified Hurricane Weather Research and Forecasting model (HWRFxUT). Hurricane Helene, which originated in the Caribbean and intensified into one of the deadliest hurricanes in recent history, provides a valuable case for exploring cold pool–hurricane interactions. The modeling framework employs nested domains at 9 km, 3 km, and 1 km resolution over the contiguous United States and incorporates a series of sensitivity experiments. In these experiments, the rainfall evaporation rate within the Ferrier–Aligo microphysics scheme is modified to 50% and 150% of the control run to assess how variations in cold pool properties influence storm behavior. The influence of cold pools on hurricane tracks is found to be negligible, whereas stronger cold pools are associated with reduced storm intensity. Their effect on hurricane-associated precipitation differs between the initiation and mature stages of the storm. Diagnostic analysis reveals that enhanced cold pools in hurricane environments increase surface latent heat flux in the outer core and lead to a general rise in surface sensible heat flux, while simultaneously reducing latent heat flux in the inner core. Additionally, stronger cold pools are linked to an expansion of hurricane size. The results demonstrate that variations in cold pool intensity can produce substantial changes in hurricane structure and evolution. These findings underscore the importance of accurately representing cold pool processes in numerical models to improve tropical cyclone forecasts and highlight the need for continued investigation into this critical yet underexplored aspect of hurricane dynamics.

Rock Physics (3 Participants)

Lambert, Isabelle., Tisato, Nicola

"Insights into Fault Roughness over the Seismic Cycle of Laboratory Earthquakes"

Booth #A-26

Earthquakes are produced by the slip events along faults driven by the accumulation and release of elastic energy in the Earth's crust. They are cyclic, and a broad spectrum of slip behaviors is observed along seismogenic faults. The irregular and chaotic nature of earthquakes makes it difficult to establish a predictive law. Furthermore, the constitutive behavior of active fault zones remains a subject of debate, particularly regarding the relative roles of static and dynamic energy controls during seismic events. Elastic energy accumulation in the crust leads to rupture nucleation, while rupture propagation and arrest are likely governed by the physical properties of the fault zone, which vary between events and evolve during slip. While numerous parameters have been proposed to influence these processes, we emphasize that fault geometry and fault–fault interactions represent fundamental controls on rupture behavior and the evolution of the seismic cycle. To better understand how the size and distribution of asperities along faults control the earthquake cycle, we conducted laboratory experiments on analog material samples with root-mean-square (RMS) roughness values ranging from 0.5 to 30 micrometers (μm). We used the Energy-Controlled Rotary Shear (ECoR) apparatus to replicate the earthquake cycle in the laboratory. The ECOR allows for spontaneous nucleation of laboratory earthquakes at velocities, accelerations, displacements, and magnitudes comparable to those observed in natural earthquakes. In these experiments, we used a loading spring with an effective elastic constant (KE) and varied the sample-averaged normal stress (n). Across experiments, we observe a range of slip behaviors, from stick–slip to steady creep, over the lifetime of the laboratory fault. We hypothesize that the size and distribution of asperities along the fault control the style of fault slip. Furthermore, over the course of the seismic cycle and in the presence of frictional weakening, we propose that the power density, another aspect that we will explore in the future, and the critical nucleation size control the magnitude of earthquakes.

Pena, Vicente., Tisato, Nicola

"Studying Gouge Pore Pressure in Stick-Slip Labquakes using the Energy Controlled Rotary Shear (ECOR): Investigating Dilation and Compaction Effects in Gouge"

Booth #A-27

Fault gouge, a granular material formed from the brittle deformation of fault rock, plays a critical role in the mechanics of earthquake nucleation. This study explores how pore pressure evolves within fluid-saturated fault gouge during and before stick-slip events. We used the Energy Controlled Rotary Shear (ECoR) apparatus, a machine that delivers energy indirectly through a spring and allows for spontaneous nucleation of labquakes. Experiments are conducted with an analog gouge material (40% silica powder, 40% glass microbeads, 20% PVC), which is used for analog modeling experiments, under controlled normal stress and water-saturated conditions. A high-

resolution data acquisition system (30 kHz) records normal force, torque, temperature, and pore pressure from a pressure sensor placed 1 mm away from the fault gouge. Preliminary results suggest cyclic compaction and dilation behavior within the gouge, with corresponding changes in pore pressure that precede and follow slip events. These pressure changes appear to change the effective normal stress on the fault interface, thereby influencing the timing and magnitude of the labquakes. Our findings support the hypothesis that fault gouge acts as both a mechanical and hydrological mediator during rupture, with direct implications for understanding natural fault behavior and refining earthquake prediction models. Future work using the ECoR will further test fluid-induced instabilities.

Myrick, Isabelle., Tisato, Nicola., Pena, Vicente

"Quantifying the Critical Pore Pressure Perturbation for Seismicity Triggering:

Experimental Insights from Fluid-Injected Rotary Shear Faults"

Booth #A-28

The injection of fluids into the Earth's crust is a fundamental driver of fault instability, whether it is controlled by industrial fluid injection or natural hydrologic loading. Yet the precise pore-pressure threshold required to trigger failure in a critically stressed fault remains unknown. Anthropogenic activities involve rapid, high-pressure injection pulses, while natural phenomena such as heavy rainfall and seasonal groundwater fluctuations can induce subtle hydrological loading that, while negligible on stable faults, may be sufficient to trigger imminent failure on those near a critical state. This study utilizes an Energy Controlled Rotary (ECoR) machine to investigate this sensitivity. We first leverage archival stick-slip data from dry crustal analogs, specifically CM2, a brittle granular composite made up of 40% silica powder, 40% glass microbeads, and 20% PVC powder, to establish a mechanical baseline, defined by a dry friction coefficient of $\mu \approx 0.5486$. As a Mohr-Coulomb material, CM2 serves as a high-fidelity analog for fault gouge by reproducing the strain-softening and plastic deformation observed in natural shallow rocks. Building on this, we propose implementing a novel modification to the ECoR apparatus featuring a graduated burette assembly designed to introduce minute pore-pressure perturbations at the fault interface that mimic both anthropogenic injection pulses and natural hydrologic cycles. By systematically bringing simulated granular faults to a critically loaded state, defined as around 99% of the previously established dry failure envelope, we will then measure the exact increment of fluid pressure ($\boldsymbol{\Delta} Pp$) necessary to initiate slip. We hypothesize that a minute pressure increase of 0.002868 MPa might be sufficient to reduce the effective normal stress below the frictional sliding threshold, reflecting the extreme sensitivity of faults near their critical state. This experimental design allows us to isolate the hydraulic triggering

mechanism from mechanical loading effects, as well as define the critical sensitivity of faults to minute pressure perturbations, providing essential data for refining constitutive laws and improving predictive models for fluid-induced seismicity in both natural and anthropogenic contexts.

Afternoon Session: 12:45pm – 3:45pm

High School Students & GeoFORCE (12 Participants)

Bakulin, Andrey; Rohatgi, Akshika; Zhang, Cameron

"Data-Driven SNR Estimation for Challenging Land Seismic Data"

Booth #B-48

In modern single-sensor land surveys, such as those in desert environments, the pre-stack signal is often buried deep below the noise floor, making visual assessment very challenging. Precise signal-to-noise ratio (SNR) estimation is important to improve from subjective data quality assessments and ensuring that noise attenuation analysis meets the absolute thresholds required for pre-stack inversion. My research project replicated the comparison of three data-driven approaches: correlation-based, stacking-based (related to semblance), and Singular Value Decomposition (SVD). By comparing these methods against controlled synthetic experiments with known SNR levels (down to -60 dB), I reviewed performance and stability by identifying the "lowest reliably estimated SNR." The research demonstrated that the stacking-based method is the most robust, offering superior stability compared to SVD or correlation methods. However, these methods face challenges as the noise level increases, because their reliability is related to the size of the trace ensemble. While Gaussian noise tests show high accuracy

with relatively few traces, realistic field noise requires significantly larger ensembles to avoid bias. To avoid this obstacle,one can increase the trace count until the SNR estimate stabilizes—as a metric to ensure the reliability and accuracy of absolute SNR quantification in real-world seismic data.

Elseifi, Kareem

"A Hybrid Data-Driven Framework for Seasonal Prediction of Accumulated Cyclone Energy along the U.S. Gulf Coast"

Booth #B-49

Seasonal prediction of tropical cyclone activity remains challenging due to nonlinear coupling between large-scale climate modes, ocean thermodynamic conditions, and regional atmospheric variability. Accumulated Cyclone Energy (ACE) integrates storm frequency, intensity, and duration and is widely used to characterize seasonal hurricane activity. This study presents a research effort aimed at predicting ACE for the U.S. Gulf Coast using Extreme Gradient Boosting (XGBoost) with physically motivated predictors, including ENSO indices, Atlantic multidecadal variability, circulation indices, and Gulf upper-ocean heat content. Two modeling configurations were evaluated using a fixed-seed 80/20 holdout split: (i) a continuous XGBoost model for ACE, and (ii) a hybrid regression-plus-binning framework that converts ACE predictions into five activity categories for risk communication. The continuous XGBoost model achieved moderate accuracy, while the binned framework provides categorical outlooks but exhibits lower validation accuracy. Forecast values for 2024–2025 were included as scenario-based illustrations conditioned on available predictor estimates. Overall, the results demonstrate that gradient-boosted decision trees can capture part of Gulf Coast ACE variability, while also highlighting the limitations of seasonal prediction at regional scales.

Solomon, Mallory; GeoFORCE

"The Importance of Understanding the Highland Lakes of Central Texas Through the Use of Sonar Technology and Sedimentary Analysis"

Booth #B-50

With an advanced lake system like the Highland Lakes, it's important to understand why key dams were built and the need for sediment samples and river mapping to support river management, environmental safety, and water resource understanding. While researching the Highland Lakes, we saw the value of using Multibeam and Sidescan sonar to map the lake bottom. We also used a Ponar to collect sediment samples from different depths and locations along Lake Austin. From data collected, closer to the Tom Miller Dam there was a higher concentration of silt and clay

with less vegetation. Upstream there was a higher concentration of sand and gravel with more vegetation. This is due to the water velocity being faster when the water is allowed to flow freely upstream, whereas when you look at the water by the dam, it is a lot slower, which doesn't allow it to carry heavy sediment. We concluded that our findings were important and valuable to the citizens of Austin because they are able to help us understand that if more silt and clay builds up by the dam, that may pose a problem to the amount of water that lake Austin can hold. Though we were not able to test our samples for microplastics due to time constraints, we were still able to understand that Lake Austin contains many micro plastics within all sediment samples which poses a problem to Austin's drinking water.

Howes, Sophia; Capetillo, Elijah; Behnke, Griffin; Lopez, Adriana; Sun, Chenguang, GeoFORCE

"Synthesizing KREEP Rocks & Analyzing Elemental Components of Lunar Geology"

Booth #B-51

True lunar samples are extremely rare and challenging to obtain. To address this, scientists fabricate synthetic lunar rocks in the lab using experimental petrology techniques. This project focuses on the formation and composition of KREEP basalts, a unique type of lunar rock enriched in potassium (K), rare-earth elements (REE), and phosphorus (P). These elements, especially REEs, are not only critical for understanding lunar geology, but also for electronics, renewable energy systems, and high-tech manufacturing. KREEP basalts are particularly important because they represent the final stages of crystallization from the past lunar magma ocean. By recreating these conditions and analyzing the resulting mineral phases, we gain insights into how the Moon's interior evolved. Our findings not only support theories of lunar differentiation, but also demonstrates how experimental petrology can model planetary processes without the need for extraterrestrial samples.

Mullins, Davis; GeoFORCE

"Using Ancient Corals to Assess Climate Simulations of El Niño Events in the Past and Future"

Booth #B-52

El Niño is an interannual weather event that heats the surface of waters in the central Pacific, causing droughts and floods across much of the planet in extreme cases. As population increases and climate change worsens, it is necessary to understand how this will affect El Niño. In order to assess the accuracy of the CESM (Community Earth System Model), which is the US' model for projecting ENSO data in the past and future, we compared simulations of climate in the model with coral proxy data of El Niño. This,

in theory, would allow us to see if the model is accurate, and either continue sampling for more data, or if the climates don't match up, to adjust the model itself. The coral we sampled was collected from the island nation of Vanuatu in the southwest Pacific, and it's about 11,300 years old, as measured using Uranium-Thorium disequilibrium, along with x-rays of the coral, revealing the underlying rings on the coral used to guide sub-sampling. We used a CNC Mill to acquire coral samples every 0.9mm representing ~1 month of time to compile a nine year record of sea surface changes in Vanuatu. Results are pending, but previously measured coral records from Vanuatu show weaker El Niño events ~12,000 years ago, agreeing with climate model simulations. This same climate model shows that extreme El Niño events will be more common in the future, providing a drastic scenario that needs to be tested with more proxy data from the past.

Trujillo, Jasmin; GeoFORCE

"ED41A-0570 Investigating the Relationship Between Shrew Diversity and Climate Change in Central Texas During the Late Pleistocene"

Booth #B-53

Inner Space Caverns serves as a unique time capsule, lending us a one of a kind view into the Late Pleistocene through the invaluable and irreplaceable fossils found within. These fossils reveal patterns from the past that can be recognized in the present. Understanding those patterns can help prepare us for the future. Our main method of discovery was analyzing the diagnostic morphology of fossil shrew teeth collected from differing depths of a debris cone in Inner Space Cavern. Next was individually classifying those specimen into one of four shrew genera, Sorex, Blarina, Cryptotis, and Notiosorex. This allowed us to link shrew diversity to certain climate intervals of Central Texas from before 20,000 years ago. Our first sample dated back to somewhere between 29,800 to 47,640 years ago and included a total of 12 specimens that we determined to have belonged to the Blarina and Cryptotis genera. This sample was collected 35-40 cm below the surface of Debris Cone 3's excavation site. Our second sample was excavated 45-50 cm below the site and contained 3 specimens that we could find, one of which we could classify as Cryptotis. While we did not have an estimated time-frame for the second sample, we know that it is older than the first because it came from a greater depth. From these findings, we were able to conclude that the Cryptotis and Blarina genera were both present during MIS-3, the climatic interval that lasted from 29,000 to 57,000 years ago. While it may be possible that the Sorex and Notiosorex were also present during that time, it was not indicated in our sample research and could be a result of sample bias. However, based on our results, our knowledge of shrew ecology, and past research, we can make hypotheses about what our findings might mean. It may be possible these shrew adapted to the warm and dry climate of MIS-3 despite it being the opposite to the cool and wet climate that is preferred by the Blarina and Cryptotis shrews.

Perhaps this climatic interval was still inhabitable enough for these shrew to survive until they were eventually extirpated during the Holocene. Regardless, these discoveries have laid the foundation of what future studies can build off of, helping us to understand how shrew diversity may have been impacted by climate patterns during the Late Pleistocene.

Raab, Lainey; Perez, Ariano; GeoFORCE

"Mitigating Climate Change Through Carbon Capture and Storage in the Subsurface of Mississippi Utilizing Economically Feasible Strategies"

Booth #B-54

Carbon capture and storage (CCS) plays an important role in addressing climate change by reducing the carbon dioxide released into the atmosphere by industrial processes. We analyzed data logs (Fig. 2) from four different wells and measured the characteristics of the Wilcox formation in Adams and Franklin counties in Mississippi. We then inputted the information into EASiTool (Fig 3,4,5) to find the most suitable and cost-efficient well details, as well as the storage of our reservoir. During this study, we were able to understand how to manage EASiTool 5.1 and strategies to compare/evaluate different financial data. This helped to determine the most feasible option for carbon capture and storage projects. Based on our results, we discovered it would take approximately 49 years for our reservoir to reach its max capacity (Fig. 3) and gaining exponential increase in investment.

Mickler, Sierra; GeoFORCE

"Radiometric Dating and Geochemistry to Explore the Possibility of Pannotia"

Booth #B-55

For decades, there have been ongoing debates regarding the existence of supercontinents from hundreds of millions of years ago, including one called Pannotia, where the present day landmasses of Antarctica and West Texas were connected to each other. Zircons, commonly found in rocks in low abundance, are crucial to finding out the age and composition of a rock. Our method of research for this project required many steps. Firstly, we acquired zircons from granite and rhyolite samples from the Franklin Mountains in West Texas and Coats Land in Antarctica. By many rounds of crushing and grinding up our rock samples, we were left with powder, homogeneous but not yet exclusively zircon. To isolate the zircons we needed, we separated that powder through density and magnetic susceptibility followed by manual picking of zircons so that all that was left to put into our mount were high quality zircons. Advanced machinery specialized for geochemistry, an excimer laser and mass spectrometer, made it possible to determine the age and composition of our zircon samples. From our analysis of select points of zircons with the mass spectrometer, we were able to see similar isotope ratios of both

lead and hafnium in both samples, which indicate similar age and composition, respectively. We selected specific spots on zircons and analyzed U/Pb and hafnium isotope ratios for a granite sample from the Franklin Mountains and a rhyolite sample from Coats Land. Through our research, we discovered that the zircons from the two samples are the same in age and composition. The similar results from these two samples is consistent that both rock samples came from the same magma source, supporting that the landmasses of Antarctica and West Texas were together when the rocks formed at ~1100 Ma. Based on the link between Antarctica and West Texas, we conclude that our results support the theory of Pannotia.

Gagrani, Suhani

"Making AI Less Thirsty: Water-Efficient Cooling and Scheduling for Data Centers"

Booth #B-56

AI-focused data centers are expanding rapidly, and even energy-optimized facilities can consume substantial freshwater for cooling. This hidden water demand matters because many data centers operate in water-stressed regions, and current scheduling tools rarely balance cooling-water impacts against energy when determining where AI workloads run. I developed a water-aware scheduling prototype that ingests data-center parameters (cooling type, power usage effectiveness (PUE), water usage effectiveness (WUE), and regional water-stress indices) and AI job characteristics (compute demand and deadlines). The scheduler assigns jobs to minimize a stress-weighted water metric while constraining total facility energy to remain within 5% of an energy-optimal baseline. To validate the water-per-energy values used in simulation, I built a bench-scale testbed with a controlled heat source, fan, and water reservoir to compare air-only and evaporative cooling. Evaporative cooling maintained lower internal temperatures than air-only cooling but consumed measurable water, confirming a temperature–water tradeoff. In multi-site simulations, an energy-only scheduler reduced energy relative to a local baseline but, in some scenarios, concentrated workloads in high-stress, high-WUE regions. In contrast, the water-aware scheduler consistently reduced total stress-weighted water use across tested scenarios while keeping total energy within the 5% cap. These results indicate that shifting flexible AI training jobs to less water-stressed sites can reduce water impacts without major energy penalties. Future work will explore reinforcement learning–based scheduling that adapts policies from operational data as conditions change.

Thornhill, Lela., Hollingsworth, Nathan., Hurles, Isla., Matula-Rees, Gavin, GeoFORCE

"The Pursuit of Earthquake Precursors Through the Lens of ECoR (Energy Controlled Rotary Shear Apparatus)"

Booth # B-57

Strike slip earthquakes like those that struck Gaziantep, Turkey and Haicheng, China, have the potential to be deadly due to lack of preparedness. Before the Haicheng Earthquake, citizens were able to prepare ahead of time due to the detection of precursors. Earthquake precursors are signs that indicate that an earthquake is about to happen. This includes seismic anomalies, which can be recreated on a smaller and quicker scale. This project focuses on several data sources to pinpoint signs of precursors, including mechanical (displacement, force, torque), video, and acoustic data, in order to study the relationship between an earthquake and preceding activity. Using the Energy Controlled Rotary Shear Apparatus (ECoR) we were able to recreate weakening and strengthening mechanisms in earthquakes by utilizing PMMA (plexiglass) to simulate granite at 20 kilometers below the surface. Various trials were performed in order to develop a large data set. After analysing the data, trial 19 was selected to be a representative trial due to precursors observed within the trial. A relationship was determined between the acoustic, brightness, and mechanical data that showed a correlation between earthquakes and precursors. Future trials as part of a larger study will be conducted in order to develop a deeper understanding of this relationship and what it could mean for the possibility of predicting earthquakes in the future.

Gonzalez Guajardo, Diego., Fakhreddine, Sarah., GeoFORCE

"Accelerated Evaporation Rates and their Far-Reaching Effects on Texan Reservoirs"

Booth #B-58

As the world grows, meeting water demand becomes increasingly difficult, making proper management essential for fair access and environmental sustainability. One of the major challenges in water control is the inevitable loss through evaporation. To better understand this issue, our research measured evaporation rates at Lake Waco, Lake Brownwood, and Lake Travis by analyzing temperature data collected from each location. We chose these lakes based on their varied temperatures, environments, and water capacity. Using Python and Daily Lake Evaporation Model (DLEM), we analyzed how climate impacts evaporation and regional water availability by creating graphs/charts. Field observations at Waco Dam and a presentation by the Brazos River Authority deepened our understanding. We found evaporation rates in August rose with higher temperatures, showing a clear relationship. Regional data revealed decreasing water levels in August, indicating that climate evaporation may contribute to droughts, extreme weather events, and unavailability for municipal purposes.

Sahoo, Sanvi., Hovorka, Sue., GeoFORCE

"Evaluating CO2 Capture and Investment Efficiency in Southwest Louisiana: Opportunity and Challenges"

Booth #B-59

As atmospheric carbon dioxide levels continue to rise, practical climate solutions are urgently needed. This project investigates carbon capture and storage (CCS) as a strategy to reduce CO_2 emissions by identifying geologically suitable underground sites for long-term storage. We employed a structure map and wirelog mapping to analyze subsurface features, with a focus on faults, elevation changes, and sandstone layers. Our findings indicate that thick, porous sandstone formations overlain by impermeable rock layers offer the most significant potential for safe and permanent CO_2 containment. These results highlight the critical role of geoscience and mapping in guiding responsible site selection for CCS, supporting global climate mitigation efforts.

Energy Geoscience (18 Participants)

Rohatgi, Akshika; Bakulin, Andrey; Fomel, Sergey

"Theory of seismic phase analysis using circular statistics"

Booth #B-1

Seismic phase is critical in imaging, inversion, and coherence measurements. However, noise contamination complicates its analysis, making reliable estimation challenging. We propose to leverage circular statistics, particularly the von Mises distribution, to provide a more robust framework for characterizing phase variations in seismic signals. Computational experiments with synthetic data demonstrate the effectiveness of this approach.

Ramadhan, Romal; Hosseini, Seyyed A.

"Sealing or Leaking? Evaluating Fault Integrity Under CO2 Storage Operations in the Gulf Coast Miocene"

Booth #B-2

Secure geologic storage of CO2 in the Gulf Coast Miocene depends on whether pre-existing faults remain sealing as reservoir pressures rise during injection. We evaluate fault integrity by quantifying potential fault-mediated leakage of brine and/or CO2 during injection and by examining how fault reactivation and evolving fault properties may alter leakage risk. We developed a coupled geomechanical-flow simulation model, dividing faults into 14 regions to track flux across fault zones. Our model incorporates differentiated geomechanical properties for confining units and reservoir intervals, along with lithology-specific capillary pressure curves for sand, siltstone, and shale facies. We examined scenarios through sensitivity analyses, varying fault mechanical properties (prone-to-fail versus more-resistant configurations), permeability multiplier tables (more-leaky versus less-leaky fault behaviors), and solubility effects. Our results demonstrate that the one fault region exhibits the highest brine leakage rates across all scenarios,

while higher Poisson's ratios in confining units produced notably distinct flux responses compared to baseline cases. The Area of Review (AoR) remains relatively consistent across scenarios, with no detectable CO2 migration to monitoring layers. We show that conservative modeling assumptions—including reduced capillary pressure values and omitting solubility effects—yield more conservative leakage estimates while significantly reducing computational time. We identify fault permeability evolution as a primary control on leakage magnitude, informing recommendations for alternative permeability-evolution assumptions in future simulations. These results support risk assessment and operational planning for geological carbon storage in faulted reservoirs.

Abu Alreesh, Mohammed; Eichhubl, Peter; Gajda, Dawid

"Geochemical Controls and Hydrogen Loss in Subsurface Storage: Evidence from Autoclave Experiments"

Booth #B-3

Underground hydrogen storage (UHS) has recently attracted interest as the transition to a clean hydrogen economy gains traction among industry stakeholders. Geochemical water-mineral-gas reactions could result in reservoir deterioration and hydrogen loss during storage cycles. To investigate these geochemical reactions in reservoir rocks under high P-T conditions mimicking subsurface conditions, we conducted autoclave experiments involving rocks, water, and H2 gas. We tested feldspar-rich Boise sandstone and single-crystal K-feldspar to quantify hydrogen reactivity. Boise sandstone and single-crystal K-feldspar samples were reacted with deionized water and an H2 gas mixture at reservoir conditions (80°C, 10 MPa) for 28 days. Water samples were collected during the autoclave experiments, demonstrating that Al precipitated more rapidly than other mobile elements, suggesting that clay precipitation occurred more rapidly than feldspar dissolution. Additionally, even at low H2 concentrations (1%), changes in pH and impacts on mineral surface reactivity and precipitation products were observed from SEM textural changes, which could affect reservoir quality. Furthermore, hydrogen loss rates were low but measurable, with sandstone showing much higher consumption rates than the single-crystal K-feldspar run. Hydrogen gas consumption was higher in the Boise sandstone experiment compared to the single-crystal feldspar experiment, suggesting that reactions with Fe-bearing clays can consume H2, particularly at higher temperatures. We conclude that H2-induced geochemical reactions vary depending on rock mineral composition and reservoir conditions; thus, the selection of suitable reservoir formations can potentially affect UHS performance.

Maulana, Bimar; Meckel, Timothy; Uroza, Carlos; Ralanarko, Dwandri

"Assessing CO2 Storage Potential within the Sunda Strait, Indonesia"

Booth #B-4

Indonesia's Net Zero Emissions 2050 target urges the need for Carbon Capture, and Storage (CCS) activity. This study will assess the Sunda Strait area in western Indonesia as a potential saline aquifer CO 2 storage in the Oligocene-Miocene Talang Akar Formation (TAF). The TAF consists of thick, porous, and laterally continuous sandstones interbedded with shales in a half-graben tectonic setting. Subdivided into the Zelda Group (Late Oligocene) and the overlying Gita Group (Early Miocene) (Sukanto, 1998), the Middle-Upper Zelda interval is designated as the primary storage target and the overlying shale-prone Gumai Formation provides as regional seal. Five wells are examined to characterize lithology, porosity, and permeability. 2D and 3D seismic data, tied to wells, were used to map the pertinent formation in order to define the configuration of the reservoir. RMS amplitude attributes are applied to delineate sand presence and distribution. Well-log interpretation reveals sandstone-dominated sequences up to 700–800 m thick. Structural mapping identifies about 52 faults, including a major half-graben fault in the east and multiple growth faults in the west. These faults likely would not pose any risk of CO 2 leakage since they are distant from the storage target. RMS attribute analysis shows the highest sandstone concentration in a central depocenter, located within the syncline which defines the most favorable zone for storage. Quantification of CO 2 storage capacity, using EASiTool (a public software developed at GCCC-BEG), will be performed with consideration of geological factors, such as area, sand thickness, porosity, permeability, and reservoir pressure.

Mensah, Shirley; Fomel, Sergey

"StrataFlux: A Machine Learning Framework for Local RGT Estimation"

Booth #B-5

Relative Geologic Time (RGT) modeling is a key component of seismic interpretation, providing a chronostratigraphic framework for understanding subsurface stratigraphy, structural architecture, and depositional patterns. Accurate estimation of RGT supports geologic characterization tasks such as horizon interpretation, stratal slicing, and identification of potential storage intervals for applications including CO2 sequestration. Traditional RGT workflows often rely on manual horizon picking or commercial interpretation tools, which can be time-intensive and challenging to scale across large or data-limited seismic volumes. Recent deep learning approaches have sought to automate RGT estimation, but many require fully labeled training data, offer limited geological interpretability, or are difficult to generalize across datasets. This research introduces StrataFlux, a machine learning–driven seismic attribute designed to estimate RGT in a scalable and geologically meaningful manner. StrataFlux operates using local, patch-based training and supports inversion to recover full RGT volumes from seismic data, drawing conceptual motivation from gradient-based stratigraphic attributes such as stratal convergence and instantaneous isochrons (Lomask et al., 2009).

By emphasizing interpretability and computational efficiency, StrataFlux provides an alternative pathway for automated RGT modeling that complements existing interpretation workflows. The proposed framework will be applied to 3D seismic data from Ghana's offshore basin to demonstrate its utility for subsurface characterization in support of CO2 storage feasibility studies. StrataFlux-derived RGT volumes will be used to guide stratal slicing, reservoir interval identification, and attribute mapping, contributing structural context for preliminary CO2 capacity assessment. More broadly, this work aims to advance scalable, ML-assisted seismic interpretation methods that enable efficient pre-screening of subsurface storage potential in underexplored basins.

Wu, Fangshuai; Liu, Gabriel Z.; Alessi, Daniel S.

"Development of lithium manganese oxides for direct lithium extraction from brine"

Booth #B-6

Global demand for lithium (Li) continues to accelerate as lithium-ion batteries are a central component of electric transportation and grid-scale energy storage, yet forecasts indicate that conventional hard-rock deposits and salar brines will be unable to meet projected demand within the coming decade. In response, alternative low-grade Li resources, such as sedimentary brines, are now attracting increasing attention in the United States and Canada. Despite the vast resource in place, the low Li concentrations and complex chemistries of sedimentary brines require Li separation technologies that are economically viable, highly selective, and durable. Ion-exchange type direct lithium extraction (DLE) materials, such as lithium manganese oxides (LMOs), are one such DLE option that enables rapid and selective Li recovery, but whose performance is highly sensitive to brine composition. We found that dissolved organic compounds and aqueous sulfide species promote reductive dissolution of structural Mn(IV), along with inherent Jahn-Teller distortion within the spinel lattice during lithiation and protonation that induces local structural instability leading to Mn disproportionation. To mitigate these degradation pathways, we systematically evaluated a suite of stabilization strategies, including the doping of the lattice with cations, surface coatings, and composite material design. Laboratory tests using brines from the Western Canadian Sedimentary Basin show that coating LMO with a nano-scale layer of zirconium dioxide shields the LMO surfaces from reactive organic species, while divalent cation doping enhances structural stability by suppressing Jahn-Teller distortion, with both approaches individually reducing Mn dissolution by 50%. Embedding LMO particles within polyvinylidene fluoride (PVDF) composites or polyethersulfone (PES) beads both immobilizes the sorbents and limits interactions with detrimental organic compounds found in brine due to the hydrophobic and oleophilic nature of the polymer matrices. As a result, these composite-stabilized LMOs can sustain over 250 Li-recovery cycles, compared with only 5-10 cycles for unmodified materials. Collectively, our results demonstrate that

chemically and structurally stabilized LMOs provide a durable, scalable, and economically viable pathway for sustainable Li recovery from brines with diverse chemistries.

Liu, Gabriel; Zilko, Steven; Benyamin, Marcus; Wu, Fangshuai; Alessi, Daniel

"Sustainable Lithium Recovery: Overcoming Brine Complexity with Regenerable Biological Binders Designed via Deep Learning"

Booth #B-7

The accelerating transition to clean energy has created a projected supply deficit for lithium, and the development of unconventional resources such as oilfield and geothermal brines may address a substantial portion of the supply gap. While the amount of lithium in these brines is vast, efficient recovery is hindered by the high salinity, presence of organic compounds and hydrogen sulfide, and low concentrations of lithium found in these fluids. To date, no extraction technologies have been proven to function economically and effectively in the complex chemistry of these industrial brines, leaving a critical gap in Li extraction technology.

Among promising extraction technologies are biological binders, including cell surface expressed engineered proteins. This research employs a hybrid biotechnological framework combining generative Deep Learning with experimental evolution. The computational workflow utilizes the computational tool RFdiffusion to generate novel protein backbones and ProteinMPNN to assign sequences, which are then structurally validated and visualized using AlphaFold. This machine learning workflow successfully generated chemically distinct binding sequences for lithium, as validated against yttrium, establishing a diverse initial library. To overcome the inability of computational models to fully predict binding energetics under complex brine conditions, candidates are subjected to multiple directed evolution cycles using the Aga1/Aga2 yeast surface display system. Cell-surface expression of binders are first experimentally verified, and variants are then isolated through Fluorescence-Activated Cell Sorting (FACS) based on Förster Resonance Energy Transfer (FRET) response.

This approach offers a distinct advantage over traditional inorganic materials, which suffer from progressive structural degradation and might require energy-intensive treatments for reuse. In contrast, the biological binders developed here can be easily regenerated at low to no net energetic cost, as the host organisms autonomously re-synthesize functional proteins, allowing for indefinite material replenishment without the energy and materials costs associated with synthetic ion-exchange resins.

Agbaje, Tolulope; Chen, Yangkang; Pham, Nam; Sansal, Altay; Fomel, Sergey

"Rethinking Seismic Data Augmentation via a Diffusion-based Generative Framework: Application of Denoising Diffusion Probabilistic Model (DDPM)"

Booth #B-8

Seismic data augmentation is widely used to improve the robustness of deep learning-based interpretation workflows; however, most existing approaches rely on simplistic transformations (e.g., flips, rotations, noise injection) or on computationally expensive physics-based forward modeling, which is often poorly aligned with the statistical characteristics of field data. These methods frequently fail to capture the joint distribution of seismic textures and structural features, limiting their effectiveness for tasks such as fault detection and characterization, where labeled examples are sparse and structurally biased. In this study, we demonstrate an approach to overcome these limitations by designing a denoising diffusion probabilistic modeling (DDPM) framework for seismic image generation. DDPMs provide a likelihood-based framework for learning high-dimensional distributions of seismic images via a forward-noising process and a learned reverse denoising process. We develop an unconditional DDPM (U-DDPM) and a fault-conditioned DDPM (FC-DDPM) to generate realistic post-stack seismic image patches, with the conditional model explicitly honoring prescribed fault geometries represented as binary masks. Three open-source field datasets are standardized via robust patch-wise local normalization and clipping to ensure stable joint training across surveys with differing amplitude scales and processing histories. The U-DDPM is trained to predict additive Gaussian noise at random diffusion timesteps using a time-conditioned U-Net backbone with residual blocks, multi-resolution encoder–decoder pathways, and skip connections. To improve sampling stability, an exponential moving average (EMA) of network weights is maintained during training and used for seismic image generation. Building on the pretrained unconditional model, FC-DDPM is obtained by transferring the U-Net weights and fine-tuning on paired seismic–fault examples; conditioning is introduced by concatenating the fault mask to the noisy input and enabling classifier-free guidance through stochastic conditioning dropout during training, followed by guided sampling at inference. This formulation enables one-to-many seismic realizations conditioned on a fixed fault geometry, providing controlled variability in seismic textures while preserving prescribed structural features. Qualitative evaluation of the results shows that unconditional samples reproduce key seismic textural patterns from the training distribution, while conditional samples maintain structural consistency with the imposed fault masks. A spectral comparison in the frequency-wavenumber (F-K) domain further supports the claim that generated realizations preserve essential spatiotemporal bandwidth and dip content. The proposed workflow provides a controllable generative mechanism for seismic data augmentation, directly relevant to improving the robustness of deep learning-based seismic-scale fault detection under limited labeled data. Training on augmented data using the proposed method will hopefully lead to better generalization across a wide range of real datasets.

Cruz, Lucero Tunjar; Sweet, Michael; Whiteaker, Timothy

“MDT/RFT Pressure Data and Trends in the Gulf Basin”

Booth #B-9

Cenozoic sediments in the Gulf are often overpressured (i.e., they exhibit pore pressures in excess of the hydrostatic gradient). This could be related to the quick deposition of muddy sediment that generates pore water during compaction that is not expelled through a well-connected sand network. Understanding the pressure regime is crucial for drilling safety, hydrocarbon exploration, and geohazard risk assessment. To investigate controls on overpressure development in the Gulf, we analyzed 265 wells from a database of 1177 wells containing well logs, RFT (Repeat Formation Tester), and MDT (Modular Dynamic Tester) pressure data from the BOEM (Bureau of Ocean Energy Management). Within this subset of wells, we detailed fluid phase, fluid contact depths, average pressure, and fluid pressure gradients at specific stratigraphic intervals. Previous studies utilized mud weight data from thousands of wells across the Gulf Basin in order to map pressure and determine the top of overpressure (e.g., Burke et al., 2012). The use of RFT/MDT pressure measurements allows a more accurate determination of the depth and stratigraphic interval where the pore pressure was observed and also avoids artifacts due to overbalanced drilling that a common in mud weight data. We created 18 pressure maps.

Swaminadhan, Sujith; Fomel, Sergey

“Implicit Neural Representation as Regularizer for Multi-Parameter Elastic Full Waveform Inversion”

Booth #B-10

With the advancement in computational resources, Full Waveform Inversion (FWI) has emerged as a powerful tool for subsurface characterization by exploiting the full wavefield information contained in the seismic data. Modern acquisition systems routinely record multi-component seismic data which can be used for simultaneous inversion of multiple subsurface parameters, such as P-wave velocity (V!), S-wave velocity (V"), and density (ρ). However, elastic FWI (E-FWI) is inherently ill-posed, leading to parameter crosstalk. The absence of a good initial model often causes conventional grid-based inversion to stagnate in local minima due to cycle skipping where predicted and observed waveforms diJer by more than a half-period. To address these challenges, we propose parameterizing the subsurface elastic properties using Implicit Neural Representation, Sinusoidal Representation Networks (SIRENs). These networks represent the elastic parameters as a continuous function of space (v!(x&), v"(x&), ρ(x&); where x& denotes the spatial coordinates). This representation imposes a strong spectral bias regularization, by encouraging the inversion to prioritize the learning of smooth, global trends before fitting high frequency events. The shared

architecture and training of the networks promote physically consistent updates, thereby reducing crosstalk. We demonstrate the proposed approach on the synthetic Marmousi model, by inverting the elastic properties starting from a 1D linear vertical gradient model. Our results show that conventional grid-based E-FWI fails to recover the macro-model trend, producing high-frequency artifacts due to cycle-skipping and parameter crosstalk. These preliminary results suggest that the implicit neural representations provide an eJective framework for initial model building for elastic media, serving as a robust starting point for subsequent high-resolution FWI updates.

Hartnett, Zach; Ko, Lucy; Flaig, Peter; Lin, Ning

"Leveraging Depleted Oil & Gas Reservoirs for Subsurface Methane Storage: An Integrated Geologic, Engineering, and Economic Evaluation for Data Center Energy Supply"

Booth #B-11

The rapid proliferation and deployment of artificial intelligence (AI) is driving a surge in data center construction across the United States; with a large share planned in Texas. This expansion is intensifying electricity consumption and creating unprecedented large-load demand. The Electric Reliability Council of Texas (ERCOT) forecasts data centers could reach 77,965 MW of total demand by 2030: an increase from an initial 2024 estimate of 29,614 MW. Meeting this growth while maintaining reliability will require additional local energy resources and storage to support secure and continuous operations. In Texas, natural gas (methane) remains a cost-effective and dispatchable fuel for powering data centers compared to many alternatives (nuclear, solar, wind, etc.). In addition to these qualities, natural gas can also be stored locally in the subsurface within depleted oil and gas reservoirs. Meanwhile, persistent natural gas oversupply in the Permian Basin has outpaced pipeline takeaway capacity, leading to high-volatile and, at times, negative gas prices at the Waha Hub. When gas cannot be economically transported, flaring excess gases becomes common. Natural gas flaring emits CO2, carbon monoxide, sulfur dioxide, nitrogen oxides, and other pollutants that adversely affect local communities and environments. In extreme cases, production is curtailed or operators may pay others to take gas. One strategy to absorb surplus supply is expanded gas-fired electricity generation for data centers. Complementary to this, subsurface storage of natural gas in depleted oil and gas reservoirs offers a potential pathway to buffer supply-demand mismatches, reduce flaring, and improve the reliability of gas supply for power generation near emerging data-center hubs.

This project evaluates subsurface methane storage in depleted oil and gas reservoirs in North Central Texas. This location was selected for two practical reasons: (1) the concentration of planned and existing data center development in the Dallas-Fort Worth (DFW) area, and (2) the presence of existing pipeline and midstream infrastructure

that can enable reliable gas delivery and cycling. To identify candidate reservoirs, S&P Global's Enerdeq database was utilized to screen Texas wells using a stepwise set of filters applied from broadest to most restrictive:

1. Location (within North Central Texas)
2. Reservoir lithology (sandstone, conglomerate, carbonate)
3. Depth (less than 7,000 ft)
4. Late-life production status (oil: <10 b/d, gas: <200 mcf/d)
5. Well density indicating a field-scale cluster of wells

Filtered wells were then grouped by specific field to identify spatial clusters and candidate fields. Clusters were ranked based on proximity to current and proposed data center projects and connectivity to existing pipeline infrastructure.

From dozens of screened options, two fields were selected as high-priority case studies: the KMA oil field (Wichita County) producing primarily from Pennsylvanian Strawn Formation and the Boonsville gas field (Jack and Wise Counties) producing from Atokan Bend Conglomerate. These fields will be assessed for methane storage suitability using three integrated criteria: geologic (core to wireline logs correlation), engineering (storage capacity, deliverability, subsurface heterogeneity, and porosity-permeability), and economic (CAPEX, OPEX, price differentials, etc.). The goal of this project is to determine whether or not local subsurface methane storage in porous media can serve as a viable option for data center energy supply in Texas.

Ali, Javid; Bump, Alex

"Classification and Calibration of Legacy Well Risks for CO2 Storage in the Gulf Coast Basin"

Booth #B-12

The Gulf Coast is a major region for large-scale CO2 storage, with over 50 projects currently in development and more than 1.1 million legacy oil and gas wells. Many of these wells were drilled before modern well construction and plugging regulations, and their documentation quality can be limited. Because legacy wells penetrate sealing formations, they are often treated as a key leakage concern in CCS risk assessment. However, different studies and papers suggest different strategies for legacy well risk classification, and there is a lack of consistency across existing frameworks. Most classifications are predominantly qualitative, often based on expert judgment, with limited quantitative grounding and limited calibration against real injection experience. As a result, CCS risk can be overestimated by treating uncertainty as failure and by screening large numbers of wells that may not be physically relevant to injection pressure or migration pathways. This study evaluates how legacy well risk is defined and screened across CCS frameworks and compares this to Class I injection practice. In Class I regulation, risk is treated as a binary question under the non-endangerment standard: if a

realistic pathway exists for fluids or pressure to migrate toward a protected underground source of drinking water, the risk is unacceptable; if not, the historical incident record, while integrity-relevant failures are relatively rare and temporally clustered. Overall, the findings support a shift toward more evidence-informed, pathway-based classification and calibration of legacy well risks for CO2 storage in the Gulf Coast Basin.

Saldana, Rosendo; Flaig, Peter; Berry, Jason

"Facies characterization and preliminary depositional systems interpretation of the Woodbine Formation in the Sasi 6 ST well, Hainesville Dome/Neuoff Field, Wood County, Texas"

Booth #B-13

The Late Cretaceous Woodbine Formation (Cenomanian) is known to comprise more proximal siliciclastic fluvial-deltaic deposits (Dexter/Freestone members) overlain by more distal marine deposits (Lewisville member). The Woodbine transitions basinward into the mud-dominated offshore deposits of the Pepper Shale. Stratigraphically, depending on location, the Woodbine unconformably overlies the Buda and is unconformably overlain by the Eagle Ford.

The Woodbine is significant for academics (e.g. sedimentologists, paleontologists, paleobotanists) because it contains fluvial-deltaic deposits that host unique Appalachia flora and fauna, as well as for industry because it serves as an oil/gas reservoir, particularly in the East Texas Basin (ETB). Unfortunately, there are relatively few publications on the Woodbine in the ETB due to the depth of Woodbine burial and the complex paleogeography controlled by uplifts and salt movement. Deformation due to the salt diapirs/domes and complex faulting also makes correlation across the ETB and outside of the ETB difficult. Describing core of the Woodbine in the ETB is significant because available core is exceedingly rare and examining facies characteristics, facies stacking patterns, and key surfaces helps identify the depositional systems responsible for sedimentation and their potential geometries, improving reservoir models and predictability.

This study showcases the initial observations and preliminary interpretations of a single core of the Woodbine (Sasi 6 ST well) from the Hainesville/Neuoff Field in Wood County, TX associated with the Hainesville Salt Dome. The lower part of the core contains abundant hummocky to swaley cross-stratified sands and current rippled sands interbedded with siltstones with a low-diversity and low-abundance trace fossil assemblage. Preliminary interpretations suggest that this part of the core represents river-dominated to commonly wave-modified prodelt and delta front deposits with some channelization, offshore deposits, and possibly a shoreface. The upper part of the core lies above a significant surface of erosion and is dominated by a thick package of upper fine-to medium-grained sandstones with trough crossbeds, current ripples, and low angle

parallel laminations. Interbedded intervals of mud rich very fine sands are seen throughout this interval and there appears to be no bioturbation. Deposits are those of channel bars with potential over bank deposits that likely overlie a sequence boundary. Shallow marine tidal and deltaic facies with some wave influence cap the core just below the Woodbine Marker. This is a work in progress for an MS thesis. Several additional core that include thick Woodbine sections, the Woodbine/Buda contact, and variable Buda deposits are known to exist and will be tied to wireline logs in a broader, ongoing reservoir analysis.

Cervantes, Anna; Maraggi, Leopoldo M. Ruiz; Moscardelli, Lorena

"Energy Storage Potential of Salt Domes in the Netherlands"

Booth #B-14

One of the most pressing global challenges today is anthropogenically driven climate change, which has intensified concerns related to energy security, fossil fuel dependence, and environmental sustainability. While recent years have seen a strong push toward clean energy, the pace of this transition has slowed due to overly optimistic ambitions, along with political uncertainty, inflation, and supply chain disruptions. Despite these setbacks, efforts to decarbonize the energy sector continue. Although natural gas has served as the backbone of electricity generation and heating systems worldwide, in today's evolving energy system, hydrogen (H2) has emerged as a versatile energy carrier capable of being produced with minimal or zero greenhouse gas emissions. To successfully establish a H2 economy, its entire value chain, particularly storage, must be further developed. Salt caverns prove to be the most suitable option for H2 storage, with more reliable characteristics than porous media. The Netherlands presents a promising case with favorable geology, extensive exploration history, and a national strategy that identifies H2 as a critical element in their energy transition goals.

Because a full energy transition based exclusively on renewable energy is rather unrealistic, and while H 2 is central to long-term decarbonization strategies, natural gas remains a dominant component of the current energy system. Therefore, to assess the feasibility and performance of underground H 2 storage, natural gas storage in salt caverns provides a well-established standard. In addition, as a transitional option, H 2 - methane blends are being considered to alleviate the weight of an automatic shift from natural gas to H 2 , while also leveraging existing infrastructure. Following the procedure outlined in Ruiz Maraggi and Moscardelli (2024), this study collects a database of salt domes located in the onshore and offshore regions of the Netherlands. These selected salt domes are then analyzed, and energy storage capacities are calculated using the CoolProp thermodynamic engine (Bell et al. 2014). Storage capacities for H 2 , natural gas, and blended systems are estimated across depths of 800–1600 m, under low, base, and high

cavern development scenarios. These findings provide valuable insights into technical feasibility, scalability, and alignment with the Netherlands' energy transition goals.

Tirmizi, Syed Talha; Foster, John; Hesse, Mark

"Finite Deformation Reacting Mixture Framework for Modelling Reactive Cracking in Porous Media"

Booth #B-15

Subsurface hydrogen storage in bedded salt formations is critical for the global energy transition due to its widespread geographic availability, yet it faces significant geomechanical risks. These formations are often characterized by a layer cake stratigraphy of halite interbedded with anhydrite. Upon contact with water, anhydrite hydrates to gypsum, generating 61% solid volume expansion (swelling) which can fracture the rock and compromise the containment of the gas in the subsurface storage. Existing modelling approaches rely on small-strain assumptions and overestimate solid volume expansion by ~30. Furthermore, these models lack the kinematic refinement to decouple reaction-induced distention from mechanical strain. They implicitly assume all volume change generates stress, neglecting the reality that reactions often consume porosity before deforming the solid skeleton.

To resolve this, we present a finite-deformation reacting mixture framework implemented using MOOSE finite-element environment. Our approach utilizes a multiplicative kinematic split ($F_s = A_s\bar{F}_s$) that decouples chemical distention from mechanical strain, ensuring that porosity-filling reactions are distinguished from skeleton-deforming stress. Uniquely, this formulation generalizes Darcy's law to account for momentum production during mass exchange in reactions. Preliminary validation against the Mandel consolidation problem and a novel "Swiss Cheese" reactive benchmark confirms the model's ability to conserve mass and momentum under large volumetric changes. Unlike small-strain approximations, which can overestimate deformation by nearly 30%, our framework accurately tracks the evolution of porosity and permeability, offering vital insights for de-risking hydrogen storage in bedded salt formations.

Talen, Eddie; Bump, Alex; Uroza, Carlos

"CO2 Storage Potential of the Corsair Trough, offshore Gulf of Mexico, USA"

Booth #B-16

The growing need for effective carbon capture and storage (CCS) solutions has highlighted the importance of identifying secure geological reservoirs for long-term CO2 sequestration. While regions rich in geological data often face risks from legacy wells,

including CO2 leakage and inflated costs, the Corsair Trough, located seaward of the Texas shelf margin, presents a unique opportunity with minimal legacy well penetrations. Despite these advantages, sparse data from limited petroleum exploration activities pose key geological uncertainties related to reservoir quality, seal integrity, and pressure dynamics. This study aims to comprehensively assess the Corsair Trough's suitability for CO2 storage by focusing on six objectives: (1) presence and adequacy of sand reservoirs; (2) injectivity capacity for multi-megaton CO2 storage; (3) pressure-limited storage potential; (4) location and impact of overpressure on the storage window; (5) robustness of confining systems; and (6) economic feasibility compared to densely drilled but nearer onshore areas. It integrates sparse well logs and seismic datasets with regional analog studies and traditional hydrocarbon exploration methods to assess the CO2 storage potential of the Corsair Trough. Procedures include well log extrapolation for reservoir characterization, seismic interpretation for structural and stratigraphic analysis, pressure modeling to define safe injection parameters, and economic comparisons between offshore and onshore CCS scenarios. This research will significantly enhance the feasibility of safe, effective, and scalable CCS solutions in data-poor environments, avoiding risks associated with legacy wells and contributing substantially to climate change mitigation strategies.

Poehl, Corbin C.; Sweet, Michael; Denne, Richard

"BOEM Lease Block Layer"

Booth #B-17

Offshore leasing in federal waters in the northern Gulf Basin began in 1954. For leasing purposes, the federal waters of the U.S. Gulf Basin are divided into 29,102 lease blocks, each measuring 3 × 3 miles. For nearly 75 years, these blocks have been leased, drilled, and used for oil production by numerous operators.

The objective of this project is to determine whether a BOEM lease block was leased and, if applicable, whether it was drilled and produced oil. The reference dataset of all lease blocks was obtained from BOEM's website. Leasing, drilling, and production information from each provided dataset was formatted into Excel using various formulas. This process created six categories: Not leased, In exclusion zone, Leased, Drilled, Drilled—unknown if produced, and Produced. These categories were then imported into ArcGIS to create a map that we could query and use with other geologic data in the GBDS (Gulf Basins Depositional Systems) Arc database.

Of the 29,102 lease blocks, 40% have never been leased because they are located in an exclusion zone, and 14% have never been leased for geologic or commercial reasons. Twenty-five percent have been leased but not drilled, 13% have been leased and drilled but are not producing, and 6% have been leased and have produced oil at some point.

Outside of the exclusion zone off the west coast of Florida, two large areas of contiguous, unleased blocks were identified. This is related to a rule that prohibits leasing within at least 125 miles of the Florida coastline to protect beaches and tourism.

Another restriction is the Flower Garden Sanctuary, where leasing is not allowed in order to protect coral reefs.

The largest contiguous unleased area is located outboard of autochthonous and allochthonous Louann Salt, south and east of the Sigsbee Escarpment. This area contains 3,326 blocks, representing 70% of the available unleased blocks. Our analysis suggests that this region has low potential for existing Cenozoic deep-water plays in the Gulf of Mexico due to a lack of salt-related structural traps. Because much of this area is underlain by oceanic crust, Mesozoic Tithonian and Oxfordian source rocks were likely not deposited here, although Cretaceous Cenomanian–Turonian source rocks are likely present. There is potential for as-yet-untested pre-salt plays associated with basement rift-related structures.

The other large area of contiguous unleased blocks is located offshore south Texas in the Bravo Trough. This area contains a thick Cenozoic section that appears to be composed primarily of muddy slope and basin deposits.

Albulushi, Ali; Janson, Xavier

"Constructing a facies volume model by integrating seismic geomorphology characterization and machine learning-based segmentation"

Booth #B-18

Seismic interpretation in heterogeneous subsurface settings is often limited by subjective horizon picking and manual facies classification, particularly in structurally complex and stratigraphically mixed systems. This research integrates seismic attribute analysis with object-based image segmentation to improve the detection, classification, and spatial continuity of seismic facies. Multi-attribute seismic volumes, including amplitude-based, spectral decomposition, and geometric attributes, were generated to enhance subtle stratigraphic and structural features. These attributes were subsequently transformed into multi-band images and segmented using object-based image analysis, allowing seismic features to be classified based on spectral, textural, and spatial characteristics rather than individual trace behavior.

The segmentation workflow reduces interpreter bias by grouping seismic data into geologically meaningful objects that better represent depositional elements and facies. architecture. Supervised classification was applied using training segments derived from well control and interpreted seismic features, enabling the extrapolation of facies trends across the seismic volume. Results demonstrate that object-based segmentation significantly improves facies boundary definition, lateral continuity, and pattern recognition compared to conventional pixel-based or manual interpretation approaches.

This integrated seismic segmentation framework provides a robust and repeatable methodology for seismic facies analysis and subsurface characterization, with applications in reservoir characterization and stratigraphic interpretation. By combining quantitative seismic attributes with image-based segmentation techniques, this study highlights the potential of data-driven workflows to enhance interpretation accuracy in complex geological settings.

Surface Processes (13 Participants)

Campbell, Ryan., Mohrig, David

"Unexpected Sediment Loading of an Urban Creek by Anthropogenic Sources: Waller Creek, Austin, Texas"

Booth #B-19

Our study focuses on sediment in Waller Creek, an urban stream entirely within the city borders of Austin, Texas. Its bedrock channel is 11-km long with a steep bed slope that ranges from 0.008 to 0.01. Waller Creek is an ideal system for studying anthropogenically derived sediment because its entire catchment is underlain by a single rock type and formation, the Austin Chalk. It is a soft fine-grained carbonate with a distinctive texture and color that makes it easy to identify and distinguish from other rock types. Waller Creek base flow is insufficient to transport any of the sediment that partially covers its creek bed. However, the creek is prone to flash flooding during intense rainfalls and stage can increase by as much as 3 m. In flood, all sediment sizes are transported, including boulders. This transport has received increased attention since construction of the 1.6-km long Waller Creek Tunnel that diverts flood water beneath downtown Austin. Sediment accumulating at the tunnel's inlet must be occasionally removed, prompting interest in its origin and motivating our study. In order to identify possible sources, we have collected observations along the entire creek length and sampled bed sediment at 7 roughly evenly spaced locations upstream from the tunnel inlet. These samples consist of grains ranging from sand to cobbles in size. Surprisingly, Austin Chalk is not the major constituent in many of these samples. Our preliminary analysis has it only composing between 20% and 60% by weight. The fraction of chalk grains is correlated with particle size; coarsest clasts are primarily chalk, while chalk sand is rare. Non-chalk grains mostly are chert, quartz, and feldspar, with lesser amounts of other limestones, glass, concrete, and plastic. Observations from thin soils resting directly on top of the Austin Chalk suggest they are not the source of the exotic sediment. Instead, the chert, quart, feldspar and other limestones are similar to commonly used landscaping materials that we have observed being delivered to the creek by overland flow during intense rains. Future work will focus on further understanding the connections between grain size and composition, as well as sources for the exotic sediment.

Cecchini, Leah., Gardner, James., Befus, Kenneth., Marneni, Neha

"Impacts of topography on the behavior of pyroclastic density currents as evidenced by downed trees by the May 18, 1980, Mount St. Helens eruption"

Booth #B-20

Pyroclastic density currents (PDCs) are one of the most destructive hazards produced by volcanic eruptions because of their incredibly high velocities, densities, and temperatures. Mitigating those hazards requires being able to accurately model the behavior of PDCs, which in turn requires understanding their dynamic pathways as they travel across the land. Because PDCs do traverse the landscape, it is expected that topography can significantly impact the pathway of PDCs. This study aims to understand topography's effect on PDC behavior through the lens of the May 18 th , 1980, Mount St. Helens, which produced a PDC that devasted 600 km 2 of forest and killed 57 people. We use a series of aerial photos captured one month after the eruption to map out the directions at which trees were downed by the PDC to use as flow markers of the PDC. Previous measurements of average downed-tree azimuths captured broad directional trends but obscured fine-scale behavior and directional variability. In this study, we resolve flow-path directions at higher spatial resolution by mapping individual downed trees according to aerial imagery on ArcGIS software. Using the resulting dataset, we derive graphs comparing the downed-tree azimuths and topography (slope and azimuth of the ground) as a function of distance along observed flow paths. These analyses show the flow exhibited both topography-independent and topography-controlled behavior across a range of topographic features. In addition, we qualitatively observe distinctive PDC dynamics that vary with distance from the vent. Future work will involve numerical modeling (MFIX and IMEX_SfloW2D models) to compare simulated and observed PDC behavior, improving identification of where and when topography influences PDC behavior and flow path at high spatial resolution.

Musser, Hayden., Johnson, Joel

"Modeling the Controls on Reverse Grading in Extreme-Event Deposits"

Booth #B-21

Reverse grading is a common but incompletely understood feature of basal tsunami and storm-surge deposits, and is sometimes observed in a wide range of sedimentological systems. However, the physical controls that cause reverse grading remain poorly understood, limiting our ability to robustly infer hydraulic forcing and sediment transport conditions from deposits.

We use a numerical suspended sediment transport model for tsunami-like flows, previously calibrated against flume experiments, to explore how grain-size properties and flow conditions affect reverse grading in deposits. The numerical model tracks individual

grains as they settle through a turbulent water column and deposit on the bed over time. Importantly, the initial condition assumes that grains of all sizes are uniformly distributed throughout the water column, representing a disequilibrium suspended transport condition that is plausible for extreme flows such as tsunamis prior to flow deceleration and net deposition. In 103 simulations, we systematically vary the mean and standard deviation of source grain size distributions, the intensity of turbulent velocity fluctuations, and flow depth. For each run, we analyze vertical sorting curves and normalized mean regressions to quantify reverse-grading characteristics and the partitioning of deposits into reverse-graded, massive, and normally-graded layers.

Our results show that reverse grading is particularly sensitive to grain size distribution variability (Φ STD) and the magnitude of turbulent velocity fluctuations, highlighting these parameters as primary controls on deposit-scale vertical sorting. Coarse-grained deposits produce little to no reverse grading, whereas finer grain-size modes are associated with steeper and more persistent reverse-graded segments. Increasing Φ STD exerts a dual control: it reduces the vertical extent of reverse grading while intensifying reverse sorting within thinner intervals embedded in thicker massive sections. Reverse grading is strongest at intermediate values of turbulence. Flow depth primarily modulates reverse grading where turbulence is sufficiently strong, exerting little influence under weakly turbulent conditions. This study provides a framework for interpreting reverse-graded deposits in natural coastal strata and for constraining the flow and sediment-source conditions that promote their formation.

Papenhausen, Liesel., Goudge, Tim

"Timelapse LIDAR Imaging and Bankline Retreat in the Lower Colorado River to Constrain Human-Induced Sources of Erosion"

Booth #B-22

Rivers have shaped the distribution of human civilization, and in turn, humans alter their morphology by modifying natural flow regimes through changes in land use (e.g., development of impervious cover) and building infrastructure (e.g., industrial water discharge, stormwater drainage systems). Urbanization of a watershed is known to increase volumes of surface runoff, decrease river baseflow, and alter erosive processes. Conventional stormwater drainage systems compound this, as they funnel runoff directly into the river, driving incision and destabilization. These land use changes and water management systems drive anomalous erosion patterns along urban rivers, such as the Lower Colorado River (LCR) in Austin, TX. This is especially prevalent in East Austin, where industrial activity has rapidly increased over the past 30 years. Here we present a study, driven by community concerns and advocacy from East Austin residents, that aims to quantify recent geomorphic changes to the LCR and identify hazards contributing to

accelerated erosion. Three sites along the LCR were selected for analysis: two heavily urbanized and populated, and one located within a nature preserve for comparison. To quantify the volumetric bank erosion, we will difference timelapse LiDAR data from the Texas Geographic Information Office. Overlaying impervious cover shapefiles, total and effective impervious cover percentages will be calculated for comparison. To assess channel morphology changes over time at a higher temporal resolution, Planet Labs PlanetScope satellite images will be used to monitor bank line retreat. Repeat field surveys and drone flights will be used at each site to assess deformation style and sediment cohesion at river bends, allowing for a more accurate comparison of erosion mechanisms between sites.

Wu, Koutian., Li, Lingcheng., Rempe, Daniella., Matheny, Ashley., Yang, Zong-Liang

"How Does Integrating Plant Hydraulics Improve Noah-MP Land Surface Model: a site study at the US-Sylvania Wilderness Area site in Michigan"

Booth #B-23

Land surface models often need better ways to show plant water transport, making results less reliable. To address this gap, we evaluated the Noah-MP land surface model with a plant hydraulics scheme (Noah-MP-PHS; Li et al., 2021) at US-Sylvania Wilderness Area site in Michigan. Unlike the traditional "big-leaf" approach in models like Noah-MP, this model uses a "big-tree" concept, incorporating plant water transport processes such as root water uptake, plant water-stress factor (β), plant hydraulic capacitance, and so on. We compared standard Noah-MP and Noah-MP-PHS simulated water-energy-carbon fluxes (latent heat, sensible heat and gross primary production, or GPP) to site observations. Results showed that Noah-MP matched observations better (latent heat flux: 0.85 vs 0.81; sensible heat flux: 0.90 vs 0.85; GPP: 0.91 vs 0.87). Both models had systematic biases, underestimating latent heat flux and overestimating sensible heat flux and GPP. Noah-MP-PHS performed slightly better for GPP statistical distributions but worse heat flux results. Both models had problems with season changes and daily cycles. This study shows that although including plant hydraulic schemes, Noah-MP-PHS needs more adjustments and calibration before operation, especially for plant water-stress and energy partitioning.

Tucker, Abigail., Sylvester, Zoltan., Lawton, Tim

"Analysis of Seasonal and Long-term Wind Variation in Cyclic Facies of the Navajo Sandstone"

Booth #B-24

Cyclicity of aeolian deposits has been documented for several decades and is interpreted as the result of seasonal changes to the local wind regime. As seasons change,

wind direction and velocity change, altering where and how much deposition occurs along the lee-slope of a dune. While cyclicity is largely recognized in aeolian outcrops around the world, modern technologies have not yet been utilized to quantitatively analyze these deposits. Cyclic deposition in the Early Jurassic Navajo Sandstone consists of the alternation of two facies. A cycle represents one year of deposition, and the two facies make one set. The first facies consist of amalgamated grain flows followed by the second facies, a wedge-shaped deposit of wind ripples and grain falls. Advancements in Structure from Motion (SfM) photogrammetry have provided new opportunities to investigate cyclic sets in aeolian stratigraphy at high resolution. This technique also offers a quantitative approach to studying cyclic facies. Using SfM to create dip-oriented orthomosaics, two outcrops of the Navajo Sandstone were mapped and measured. The true thickness of the cyclic facies was measured along each of the outcrops. The first outcrop, located north of Kanab, Utah, is where cyclicity was first described in 1983 and displays two types of cyclicity. The second outcrop, located within the Grand Staircase Escalante National Monument, may indicate a higher order of cyclicity present. Thickness variations of cyclic sets may reflect a hierarchy of controls influencing deposition, with low-order controls representing yearly seasonal wind changes and high-order controls reflecting longer-term changes.

van der Maal, Camila., Mills, Tanner., Flemings, Peter

"Interpreting Depositional History from the Petrophysical and Sedimentological Characteristics of Ooze Deposits in the Deepwater Gulf of Mexico"

Booth #B-25

The Gulf of Mexico Deepwater Hydrate Coring Expedition (UT-GOM2-2) drilled and cored to a depth of 861 meters below the seafloor within the Terrebonne Basin. We encountered 5 cycles of mud and calcareous ooze from 4.5 to 152 mbsf. In SEM images, the ooze is dominated by coccolith shells. X-ray diffraction (XRD) data suggests that the cleanest examples of calcareous ooze are composed of 34% , 38% clay, 14% quartz and 6% dolomite. Particle size analysis shows that the ooze is a silty clay dominated by ~3 micron size coccoliths. The clean ooze examples have a high porosity ranging from 60 to 70% in moisture and density (MAD) measurements. In contrast, SEM imaging shows that the mud is composed of smectite-illite grains and silt sized quartz and carbonate grains. XRD data suggests that the mud is composed of 11% , 49% clay, 19% quartz and 10% dolomite. Particle size analysis shows that the mud is a silty clay dominated by smectite-illite grains smaller than 2 microns. The mud has a lower porosity ranging from 52 to 65% in MAD measurements. I interpret that the ooze is deposited as a mixture of turbidite deposits and the accumulation of coccolith tests settling out of the water column. I interpret that the mud is deposited as a series of turbidity flows. One interpretation of these lithologic cycles is that they represent the depositional response to

the 100,000 eustatic sea level changes associated with glacial-interglacial cycles that dominated the last 1 million years.

Zaleski, Danielle., Olariu, Cornel.,

"Microplastic and macroplastic dynamics along a barrier island: Matagorda Peninsula, TX"

Booth #B-26

Each year, around 400 million tons of plastic waste is produced, and 15% of that is mismanaged, ending up in the environment. As plastics are sourced on land and are transported via runoff and the atmosphere, they must move through coastal environments in order to reach the ocean (theorized as the ultimate sink for plastics). Coastal sediment dynamics and final microplastic transport mechanisms to the ocean are critical to unravel the land-to-ocean plastic flux. Studies suggest that marine plastics concentrate near the coastline at years- to decade-long time scales. Matagorda Peninsula, located at the Texas coast, is a 74 km (46 mi) long barrier island. The western Matagorda Peninsula has little anthropogenic influence and it is ideal to understand coastal micro- and macroplastics dynamics. Data from 20 sediment samples across 5 beach transects, and drone images from 4, 15, and 30 m altitude, were analyzed to understand the distribution of plastic debris along a dissipative beach setting. We hypothesize that microplastics (< 5 mm) will be most abundant at the landward extent of the swash zone, as they will be deposited as the wave energy dissipates/infiltrates the sand. For macroplastics, we hypothesize that they will accumulate near organic flotsam, getting trapped in the vegetation. Preliminary results show that macroplastic debris indeed associates with flotsam and is more prevalent in the storm berm to front of the vegetated dune area. The microplastics show a weaker trend across beach profiles, possibly because they are easily remobilized and affected by aeolian transport.

Young, Duncan., Paden, John., Yan, Shuai., Kerr, M.E., Sungh, S., Vega González, A., Kaundinya, S.R., Greendaum, J.S., Chan, K., Ng, G., Buhl, D.P., Kempf, S.D., Blankenship, D.D.

"Coupled Ice Sheet Structure and Bedrock Geology in the Deep Interior of East Antarctica: Results From Dome A and the South Pole Basin"

Booth #B-27

The deep interior of the East Antarctic Ice sheet likely contains important records of climate and ice sheet evolution. Here we report on a recent aerogeophysical survey of the southern flank of Dome A, over South Pole Basin. We find an extensive radioglaciologically defined basal unit under Dome A that abruptly truncates within South Pole Basin. This truncation aligns with a change of subglacial bed properties and distinct subglacial landforms. We infer that this basal unit may be slowly transporting and

depositing material through local basal melting in South Pole Basin into an extensive, subglacially forming, sedimentary basin. In turn, this sedimentary basin may induce locally enhanced melting by hosting local groundwater.

Guenther, Eric., Magruder, Lori., Goudge, Tim

"Characterizing the Effective Footprint Diameter of ICESat-2 when Terrain Canopy"

Booth #B-28

ICESat-2 is a critical tool for measuring and monitoring canopy heights and allometrics globally, especially beyond 51.6°N and 51.6°S. The onboard Advanced Topographic Laser Altimeter System (ATLAS) uses a gaussian beam, meaning most of the laser's power is concentrated in the center of the laser footprint. Prior work identified the footprint diameter of ICESat-2 is approximately 11 m, based on analysis of ICESat-2 measurements on an array of corner cube reflectors at White Sands Missile Range. However, the effective footprint diameter of ICESat-2 when measuring natural, more diffuse targets (including sediments) in other parts of the world is less well understood. This work seeks to better understand the effective footprint diameter by comparing ICESat-2 measurements of natural targets to high-resolution, discrete return airborne laser scanning data over boreal forests. Preliminary results indicate that the effective footprint diameter of ICESat-2 when measuring diffuse targets may be significantly less than 11 m diameter. Understanding the effective footprint diameter could improve validation techniques and enable more accurate high-resolution applications for ICESat-2, such as high resolution digital terrain maps.

Jimenez, Marcos., Malkowski, Matthew., Olariu, Cornel., Hess, Thomas

"Quantitative Seismic Morphology of Cretaceous Nanushuk-Torok Clinoform Geometries in the Colville Basin: Implications for Margin Evolution and Depositional Patterns"

Booth #B-29

The three-dimensional architecture of the Nanushuk Torok clinoforms remains an active area of investigation. In the Colville foreland basin of the North Slope, Alaska, the Cretaceous Nanushuk Torok formations comprise high relief shelf edge clinoforms that have been studied for decades, largely using 2D seismic data. Newly available 3D seismic volumes and well logs from the Colville Basin provide an opportunity to investigate shelf margin dynamics. Here we analyze 23 clinoforms grouped into 19 clinothems and document systematic changes in seismic morphology and depositional systems as the 800 m to 1000 m high (locally ~1000 m) shelf to slope clinoforms prograde northeastward. Mapping reveals two main stages of basin margin clinoform evolution, consistent with changes in sediment supply, accommodation, and

sedimentary processes that partition sediment across the shelf slope profile. Stage 1 is characterized by thick, gently dipping (~1.5 to 2.5°) clinoforms that initially resemble a ramp style margin with combined shelf margin aggradation up to ~280 m and progradation over ~2.5 km. Stage 1 then evolves into a margin with predominantly flat shelf trajectories extending over ~20 km, multiple sinuous downslope migrating channels (>100 m wide), direct sediment bypass to basin floor lobes, and an absence of large submarine canyons in the mapped area. The lack of canyons suggests a direct fed margin in which shelf edge deltas connected to basin floor fans via slope channels, comparable to shallow, underfilled basins and epeiric settings such as the Western Interior Seaway. Stage 2 records a progressive transformation to a thinner, steeper (>2.0°) and locally oversteepened margin. An early transitional phase is marked by a relatively fixed shelf edge position and up to ~180 m of shelf margin aggradation, consistent with a constructive margin style, development of well imaged lobate shelf edge deltas, and initiation of gully incision at the shelf slope transition. This is followed by a fully developed stage characterized by deeply incised gullies and fewer slope channels, rugose slope profiles with along strike linear sediment waves(?) on the lower slope, and repeated slump deposits. These features are consistent with enhanced slope instability and shelf edge failure and may represent early stage processes associated with the large scale Dalton Slide mass transport complex in the study area. Stage 2 resembles well documented shelf to slope margins with thick shelf edge delta depocenters and multiple sediment conduits described from foreland basins such as the Washakie Basin, as well as other tectonically influenced margins where mass wasting processes influence shelf edge evolution. The preserved evolution of the Nanushuk Torok margin reflects the influence of high sediment supply, a deep foreland basin, and structural inheritance associated with the Barrow Arch that created conditions for basin margin clinoforms to pass through and preserve key morphological stages of basin margin build out. These results document high resolution source to sink relationships in deep water sedimentary systems applicable to basins with comparable tectonic frameworks, and they improve prediction of the spatial distribution and controls on Nanushuk Torok reservoirs within the Colville Basin.

Paramita, Valina Rizky., Olariu, Cornel

"Tidal Controls on River Geometry: a case in the Papua Island setting"

Booth #B-30

Research on tidal-influenced deltas has largely been descriptive, with quantitative efforts dominated by modeling. A systematic quantification of modern delta geometry remains scarce. To address this gap, we analyze the geometry of rivers that feed Holocene tidal-dominated deltas in the Papuan Fold Belt zone setting. The rivers are the Fly River, Bumu River, Turama River, and the Digul River. These rivers are known for their high sediment influx and mesotidal influence conditions. Moreover, spring tides in

this area can reach up to 2.8 meters. The focus of this study is on measuring river geometry along a transect from the delta shoreline landward. We quantify the relationships between tidal range and two geomorphic metrics: the river-width ratio and the river-width-change. The river-width ratio is the ratio of the river width to a river width in a reference point, while the river-width-change is the delta value of the river width in unit length. The results show the river width increases toward the shoreline, and the river-width-change decreases landward at a rate of 0.04. These findings provide a clearer picture of the tidal imprint on delta distributary channel geometry, offering transferable constraints for reconstructing paleogeomorphology and tidal influence in ancient delta systems. Furthermore, a global-scale comparative analysis across diverse tidal systems is needed to refine these relationships and yield more representative parameters for ancient reconstructions, subsurface analogs, and hydrocarbon reservoir models.

Murphy, Kalen., Sylvester, Zoltan., Covault, Jacob

"Minibasin Turbidite Deposite"

Booth #B-31

Turbidites can record geological and atmospheric events from sediment transport out to the deep sea. Turbide deposits are typically normally graded event beds with thick sand at the base and thin mud on top. In minibasins, the sediment is confined creating a thicker sand and thick mud cap. Basin IV is a salt-withdraw minibasin that is within the Trinity–Brazos system off the Texas coast, which has a large turbidite deposit due to ponding. This minibasin has a ~40m large turbidite deposited in the Late Pleistocene with a ~17m mud cap.

Here we used the U1320 core from IODP, sediment samples from the core, LPSA, and seismic-reflection data to explore and interpret the depositional process of the turbidite deposit. The purpose of this project was to reinterpret the previous analysis of the core and the turbidite and the proposed mud layer within the sand unit of the deposit. We interpret this as a mud clast as comparing the other cores drilled in the basin, due to the ponded deposit.

Solid Earth & Tectonic Processes (11 Participants)

Muller, I.P., Ketcham, R.A., Brichau, S., Barbarand, J., Noiriel, C.

"Fully 3D Visualization and Measurement of Fission Tracks in Apatite"

Booth #B-37

Traditional fission track analyses are based on 2D microscopy, which presents significant limitations in accurately measuring and characterizing fission tracks –

particularly confined tracks, which are critical for determining thermal histories but are often scarce and time-consuming to identify in 2D. Synchrotron-based X-ray computed tomography (CT) enables the creation of 3D models of mineral grains with sub-μm resolution. This new approach not only increases the number of measurable tracks but also provides more complete shape information and crystallographic sampling.

Here we present the first 3D CT reconstructions and measurements of etched fission tracks in apatite, using data obtained at the Paul Scherrer Institut (PSI, Switzerland). Single grains were etched for 0, 20, or 30 seconds and then imaged at resolutions averaging 0.1625 μm. Dragonfly software was used to visualize the data and measure confined track lengths, shapes, and orientations. We have measured over 100 confined TINT fossil tracks in a single grain, suggesting the possibility of single-grain thermal history analysis.

In typical 2D apatite fission track studies, confined track orientations are limited to being close to the polished prismatic plane being observed through the microscope. 3D CT data provides tracks at all crystallographic angles, including some that have not previously been available or studied. We thus measure the angle of confined tracks with respect to both the c and a crystallographic axes, to pave the way for testing whether c-axis projection needs to be enhanced to account for tracks at 10-30° off an a axis. Similarly, 3D track shapes will allow further refinement of our understanding of track etching structure.

Preece, Madison., Stockli, Daniel., Thigpen, Ryan., Gallen, Sean

"Insight on recent tectonic deformation in the central Himalayan provided by fluvial terrace geometries"

Booth #B-38

Topography is a direct manifestation of the coupling of tectonic and surface processes and this connection between rapid erosion and high uplift rates is most readily evident in the frontal High Himalayas– an area that provides an excellent opportunity to study the progressive evolution geomorphic features in response to the interplay of these processes. An abrupt topographic break between the low-relief Lesser Himalaya and the high-relief Greater Himalaya has received significant attention, but the processes that govern its evolution remains debated. While it is commonly accepted that active tectonics are required to produce the topographic break, it remains debated whether it is driver by a blind mid-crustal ramp or discrete thrust faulting that daylights at the mountain front. Evidence for out-of-sequence thrusting has been documented along the orogen at similar elevations as the topographic break, suggesting active surface faulting could play a major role in generating and sustaining this marked topographic break. In central Nepal, where the topographic break is most pronounced, thermobarometric data indicate pronounced differences in maximum pressure temperature estimates (>300°C, >4 kbar)

experienced by juxtaposed Greater Himalayan units. Consequentially, this structure likely plays a major role in accommodating shortening within the orogen, which is expected to build significant topography. In the Annapurna region, this boundary lacks a thick mylonitic shear zone, suggesting that it may have experienced recent brittle activity. This study investigates neotectonic offsetting and warping of fluvial terraces that record recent thrust activity within the past tens of thousands of years. Newly available two-meter resolution digital elevation data coupled with field observations, provide an unprecedented opportunity for identifying neotectonic deformation of fluvial terrace geometries across the topographic break. We present terrace tread data from the Seti river drainage in central Nepal. An important limitation, however, is that these digital elevation data allow for detailed imaging of terrace tread deposits, rather than bedrock strath terraces, and thus are also influenced by sedimentation processes. We present preliminary interpretations based on first-order changes in terrace tread geometries over kilometers distance, ensuring that evidence is recorded across multiple terrace levels, and in some cases supported by additional bedrock data. Seti River terrace tread profiles suggest divergence upstream of the topographic break, which can be caused by differential uplift or changes in sediment flux. Multiple terrace levels also appear folded near the structural position of the Chamrong thrust, mapped in the neighboring Modi Khola drainage. At this location, we also report evidence of pervasive brittle bedrock deformation. The combination of these features suggests possible tectonic deformation at multiple locations along the Seti River that are consistent with active brittle out-of-sequence thrusting along the mountain front. We plan to combine these data with UAV models of strath terrace geometries to clarify these preliminary interpretations.

Bennett, Christina M., Martin, Craig R., Stockli, Daniel F

"Multi-Method Geo- and Thermochronologic Constraints on the Timing of Deformation and Exhumation in the Shyok Suture Zone, Ladakh, India, NW Himalayas"

Booth #B-39

Understanding the structural and temporal evolution of suture zones is essential for reconstructing the closure of ocean basins, terrane accretion, continental collision, and ophiolite exhumation during orogenesis. In the northwestern Himalayas, it has been proposed that the Kohistan-Ladakh arc formed on the Eurasian margin and rifted southward in the Late Cretaceous, opening a back-arc basin between the arc and Eurasia. The Shyok suture zone in Ladakh, India, preserves a record of the northward subduction of this back-arc basin and the collision of the Kohistan-Ladakh island arc with the Eurasian margin. However, the sequence and timing of thrust faulting within the Shyok suture zone remains poorly constrained, along with the exhumation history of suture zone ophiolites. This study presents new multi-method U-Pb geochronology (zircon, titanite, apatite) and zircon (U-Th)/He (ZHe) thermochronologic results integrated with structural

observations of major thrusts to analyze the timing of compressional deformation in the Shyok suture zone. We will focus on the thermal history of hanging wall exhumation to reveal how multiple phases of shortening have affected the structural architecture of the suture zone. U-Pb dating of titanite and apatite preserves the protolith crystallization ages despite penetrative ductile shear, suggesting that shearing took place at temperatures <450°C. The ZHe system, with a closure temperature of ~180°C, provides an opportunity to bracket episodes of brittle deformation in upper crustal thrust sheets. Comparison of ZHe ages from thrusts across the Shyok suture zone allows us to determine the timing of collision-related deformation and the influence of continuous shortening on the evolution of suture zone thrust systems. These constraints have implications for continental suturing processes, the exhumation of ophiolites in orogenic belts, and the tectonics of the India-Eurasia collisional system.

Ehrenfels, Maximilian., Stockli, Daniel F., Martin, Craig R., Stockli, Lisa D., Patterson, Desmond

"Laser-Ablation (U-Th)/He Dating of Chromite and Magnetite in Serpentinized Shear Zones: A Novel Approach to Constrain Continental Collision Events"

Booth #B-40

Chromium spinel (incl. chromite) and magnetite, abundant in ultramafic rocks and serpentinites that commonly lack mineral phases for geo- and thermochronometry, offer a promising archive for reconstructing the timing and thermal conditions of ophiolite emplacement and tectonic activity along continental suture zones. While conventional magnetite and chromite (U-Th)/He chronometry has been successful applied to dating of basalts, serpentinites, and kimberlites, these attempts encountered significant obstacles. These include uranium-rich inclusions, helium implantation into grain rims, and difficulties in distinguishing multiple growth phases within individual grains. In order to overcome these analytical challenges, we have developed methodologies for laser-ablation magnetite and chromium spinel (U-Th)/He dating at UT Austin's UTChron Laboratory, using in-vacuo laser-ablation and ultra-low-blank magnetic-sector noble gas mass spectrometry for He, a laser-ablation ICP-MS Element2 system for U and Th, and a Bruker white light interferometer for ablation pit volume measurements. The method enables ~100 μm resolution and ~10% analytical precision, allowing targeted analysis of discrete growth zones and complex intra-grain textures.

We applied this methodology to serpentinites within the Indus and Shyok Suture Zones (ISZ and SSZ) in Ladakh, India. Constraining tectonic activity along these sutures is crucial for accurately determining the timing and dynamics of the final collision between India and Asia. Electron microprobe mapping reveals complex chromite–magnetite intergrowths, including ferritchromitization at chromite rims and magnetite infilling along fractures and rims. Preliminary in-situ (U-Th)/He analyses of chromite

capture distinct phases of cooling, while magnetite records the timing of late-stage brittle back-thrusting. Simultaneously acquired mayor and trace element data provide additional information about origin and formation temperature of the dated grains. Our results demonstrate the significant potential of laser-ablation (U-Th)/He dating of chromite and magnetite to resolve complex tectonic histories and improve our understanding of continental collision dynamics, particularly in settings where conventional geochronometers are absent.

Peng, Hongrui., Mao, Shujuan

"Revealing Shallow Subsurface Dynamics through Four-Dimensional Seismic Velocity Monitoring in the Eagle Ford Basin, Texas"

Booth #B-41

Located in South Texas, the Eagle Ford (EF) Basin has experienced intensive unconventional oil and gas production since 2008, as well as irrigation since the last century. The associated anthropogenic activities, such as hydraulic fracturing, wastewater disposal, and groundwater pumping, compounded by natural precipitation variability, have continuously modified the region's subsurface stress state and medium properties. Their cumulative impact is reflected in increased seismicity and land subsidence in recent years.

To characterize these dynamic processes, we conduct time-lapse seismic velocity monitoring in the central EF Basin using continuous ambient noise records from ~30 seismic stations operating since 2019. We employ ambient field interferometry and advanced coda-wave imaging to monitor subtle changes in seismic velocity (dv/v) over time and space. We apply multiple stacking and denoising strategies to suppress incoherent perturbations in cross-correlation functions (CCFs) and improve the reliability of dv/v time series. The spatial distribution of these changes is imaged through tomography methods based on recently developed coda-wave sensitivity kernels.

Our analysis reveals pronounced spatiotemporal variations in dv/v across the Eagle Ford Basin. At mid- to low-frequency bands, dv/v time series exhibit clear seasonal to interannual variability, which correlates with groundwater-level records and surface deformation measurements, suggesting a strong hydrologic control on seismic velocity changes. On the other hand, the spatial distribution of dv/v variations is highly heterogeneous and is strongly modulated by geological structures, particularly major fault systems. Together, these observations underscore the potential of dv/v monitoring to disentangle coupled shallow subsurface processes in structurally and hydrologically complex settings.

Casazza, Mitchell., Stockli, Daniel., Stockli, Lisa., Hennings, Peter

"U-Pb Geochronology of Syn-Kinematic Calcite from the Sawtooth Mountains,

Montana – Implications for the Temporal and Kinematic History of the NW Montana Disturbed Belt"

Booth #B-42

Progression of deformation in fold and thrust belts is commonly constrained through correlation with foreland basin deposition. While this approach provides indirect timing constraints, it lacks the resolution required to discern the precise timing and sequence of thrusting events. In the Disturbed Belt of Montana, broad temporal constraints have traditionally been provided by relating thrust related deformation to both the foreland basin stratigraphy and cross-cutting igneous intrusions. The Sawtooth Mountains of Northwestern Montana are a world class example of an imbricate stack of early Paleozoic carbonate thrust sheets, which are thought to have formed largely by in-sequence thrusting. Further North, the Lewis Range in the Glacier National Park area is home to the dramatic Lewis Thrust that places Mesoproterozoic rocks over Mesozoic foreland basin strata. Despite their prominence as classic examples of thrust faulting, the timing of displacement along the Lewis Thrust and the imbricate stacking in the Sawtooth Mountains remain ambiguous. For this study, we systematically documented brittle structures associated with thrust fault emplacement and sampled syn-kinematic calcite for U-Pb geochronology. We targeted calcite slickenfibers on major and subsidiary thrust faults, recrystallized calcite in fault cataclasites, and calcite-filled tension gashes tied to fault-bend folding in the Sun Canyon and Glacier NP areas to directly constrain fault activation and refine regional kinematic models, thrust imbrication, out-of-sequence motion, and Cenozoic extensional overprinting. Despite analytical challenges posed by low U content and incorporation of common Pb, preliminary U-Pb data yielded promising results that constrain Late Cretaceous to Paleocene contractional deformation and Cenozoic extensional overprinting, suggesting a more complex kinematic history. Field relationships and these early geochronologic results hint at episodes of out-of-sequence thrusting and significant Eocene and younger extension. By integrating calcite U-Pb dating with micro and macro-structural analysis, this research is refining the tectonic evolution of Montana's Disturbed Belt, offering insights into the temporal dynamics of thrust belt formation. This study illustrates the overall power of an integrated structural geochronology approach applied to brittle deformation to elucidate the temporal and kinematic evolution of carbonate-dominated fold and thrust belts and the potential to understand fundamental linkages between progressive structural thrust belt evolution and foreland basin deposition and basin architecture.

Parker, Ema Linnea., Avendonk, Harm Van., Bangs, Nathan

"Along-Strike Variations in Oceanic Crust Formation During Continental Breakup: Basement Roughness from the Carolina Trough to the Blake Plateau"

Booth #B-43

The eastern North American margin crust shows strong along-strike variations in how continental breakup progressed during the Jurassic opening of the central Atlantic Ocean. The Blake Plateau appears to be a volcanic plateau, whereas the adjacent Carolina Trough to the north consists of rifted continental crust,yet the processes responsible for this contrast in early oceanic crust formation remain poorly understood. Previous studies suggest that the Blake Plateau experienced greater magmatism and less extension than neighboring margin segments, but a lack of direct observations of basement structure limits definitive conclusions. In this study, we use igneous basement roughness as a simple metric to evaluate how the volcanic accretion style along the northern Carolina Trough varied with distance from the Blake Plateau. Basement roughness reflects short-wavelength relief of the basement surface and provides insight into the relative roles of faulting and magmatic construction during oceanic crust formation. We present a preliminary comparison of basement roughness along two seismic reflection profiles across the Carolina Trough: one located 100 km north of the Blake Plateau and a second profile 600 km north of the Blake Plateau. We interpret differences in basement roughness between these profiles as reflecting spatial variations in crustal formation processes associated with proximity to the Blake Plateau. Initial observations show smoother oceanic basement near the Blake Plateau than along the northern Carolina Trough, consistent with a shift toward greater magmatic influence that may reflect higher mantle temperatures at the Blake Plateau during Jurassic rifting. Ongoing work will extend this analysis to additional profiles and quantitative roughness measurements to evaluate changes in lithospheric strength and magma supply along the margin.

Karaesmen, Mehmet Ege., Lavier, Luc., Taylor, Frederick

“High-resolution Coral Geodesy in the Solomon Islands”

Booth #B-44

The classical earthquake cycle is commonly described as alternating between long periods (decades to centuries) of interseismic locking and brief episodes (seconds) of coseismic rupture. However, increasingly dense geodetic observations from recent megathrust earthquakes reveal a more complex spectrum of transient deformation processes that challenge this binary framework. The New Georgia Group in the Solomon Islands provides a unique natural laboratory to investigate these processes, where the Woodlark Basin subducts beneath the Solomon Arc and has generated large megathrust earthquakes, including the 1936 Mw 7.9 and 2007 Mw 8.1 events.

The close proximity of the islands to the trench allows Porites corals to serve as high-resolution recorders of vertical ground motion. While coral morphology has long been used to identify coseismic uplift, we introduce a novel approach that combines coral morphology with stable isotope analysis (δ13C and δ18O) to quantify relative sea-level

(RSL) variations at annual resolution. We first assess the robustness of the relationship between coral water depth and δ13C using 141 new samples collected across a range of depths formed within the same time interval. For depths between 170 and 110 cm below sea level, δ13C exhibits a strong linear correlation with water depth (R2 = 0.982), while shallower samples display a non-linear response.

We then apply this RSL proxy to a 692-sample coral time series spanning 1928–2012 and validate the reconstructed RSL against available tide-gauge records. The 2007 Mw 8.1 earthquake is clearly resolved, with coral morphology recording ~70 cm of coseismic uplift expressed as a pronounced die-down surface, accompanied by a δ13C excursion exceeding 2‰. The 1936 Mw 7.9 event is similarly captured by a distinct δ18O anomaly, with postseismic relaxation observed consistently along two independent drilling transects.

Beyond discrete coseismic signals, the record reveals multi-year to decadal periods of uplift and subsidence that we interpret as complex interseismic deformation. In particular, we identify intervals consistent with slow slip activity during 1955–1964, 1977–1986, and 1999–2002. These results demonstrate that stable isotope measurements in corals provide a powerful bridge between instrumental geodesy and paleoseismology, enabling a continuous, high-resolution view of subduction-zone deformation and stress evolution across the full earthquake cycle.

Cook, Susie., Stockli, Daniel., Stockli, Lisa

"Petrochronology of Composite Footwall Mylonites in the Whipple Mountains Metamorphic Core Complex"

Booth #B-45

Characteristic of large-magnitude extension in myriad geodynamic frameworks, Metamorphic Core Complexes (MCCs) feature low-angle normal faults (LANFs), ductile footwall mylonites, and brittle distended hanging-walls. Despite their significance, our understanding of the influence of inherited structures and anisotropy on deformation in both the ductile and brittle regimes in MCCs is often poorly resolved. The Whipple Mountains MCC (WMCC) has been central in our foundational knowledge of the temporal, geometric, and kinematic development of MCCs. The WMCC is one in a series of corrugated MCCs in the Colorado River Extension Corridor (CREC) which experienced multiple phases of shortening and extension between Mesozoic shortening and most recent MCC exhumation during Miocene extension. End-member explanations of footwall mylonitization in the WMCC range from entirely syn-Miocene extension to the exhumation of earlier mylonitic fabrics coeval with regional Mesozoic/Cenozoic tectonics (e.g. Laramide). Given evidence of the latter in neighboring CREC MCCs, this high-resolution study documents the heterogeneous lithologies and strain distribution in multiple outcrops and looks at individual mylonitic facies through the lens of

petrochronology to distinguish temporal and rheological evolution of the composite rheological fabrics. We expect to find that while low-temperature (<450°C) mylonites relate to ductile shearing during Cenozoic regional large-magnitude extension and MCC formation, that high-temperature (>450°C) mylonites exemplify the capture of a preexisting mylonitic zone unrelated to Miocene extension. This preliminary data provides new insights, corroborating that Mesoproterozoic metamorphic footwall rocks were heavily infiltrated by late Cretaceous plutons and dikes (~72 Ma). Importantly, new apatite U-Pb ages fall into two distinct Eocene and Oligo-Miocene age groups, clustering at 23-28 Ma and 33-44 Ma respectively. These data indicate that high-temperature mylonites appear to be Laramide in age while lower-temperature mylonites and rocks at shallower structural levels are associated with Miocene extension and MCC exhumation. While there is ample regional evidence for Eocene and Oligo-Miocene ductile shearling, this systematic study integrating microstructural fabric analysis and zircon, apatite, and titanite U-Pb petrochronology demonstrates the composite nature of WMCC footwall mylonites and helps explicate the impact of inherited fabrics on mylonitization in MCC exhumation and answer important questions regarding the thermal and mechanical evolution of large-scale crustal extension.

Horne, Elizabeth., Hennings, Peter., Stockli, Daniel., Horton, Brian

"Anatomy of a Proterozoic Fold and Thrust Front in Far West Texas Revealed by 3D Seismic Reflection Data: Implications for Rodinian Assembly"

Booth #B-46

The Mesoproterozoic Grenville Orogenic Belt extends from northeast to southwest along the southeastern margin of Laurentia, including southeastern Canada, the Appalachians, the east-central United States, and into Texas. The structural and temporal evolution of this system has been constrained along portions of this collisional belt. However, a holistic understanding of the anatomy of this collisional margin is poorly understood due to limited outcrop exposures and tectonic overprinting from multiple deformation events spanning 1000 M.y., which resulted in the exhumation and erosion of existing structures and burial below Phanerozoic sedimentary basins. In Texas, our understanding of Grenville deformation is limited to isolated outcrops, where individual components of the collisional belt are observed including the high-grade metamorphic core of the Llano Uplift (distal hinterland), lower-grade, polyphase shearing in Van Horn (fold and thrust front), and syntectonic strata in the Franklin Mountains (undeformed foreland).

We employ a high-quality 3D seismic reflection dataset spanning >1,500 km2 of the western Delaware Basin, south of the Texas/New Mexico border that images a uniquely complete contractional tectonic assemblage below the Great Unconformity indicative of present-day north-directed tectonic transport. Specifically, the data

images kinematically linked structural elements including, from north to south, undeformed to variably shortened foreland strata with sedimentary growth geometries, an imbricate thrust belt, and a less coherent, overthickened hinterland. We believe these elements represent the frontal portion of the Grenville orogenic belt. Like the cuspate thrust salients of the Ouachita Orogeny that extended inboard

onto North America, we interpret this newly imaged frontal thrust belt as a tectonic salient that extends into southeastern New Mexico and thus places the actual tectonic front ~100 km farther north than previously mapped. We provide a preliminary interpretation of this system, relate the scale of features described to other studies along the Grenville Orogenic Belt, and provide a model for how these features may fit into the plate-scale framework of the Laurentian margin during Rodinian assembly.

Nistor, Claudiu., Barnes, Jaime., Dragovic, Besim., Gevedon, Michelle., Stockli, Daniel., Hams, Jake

"A Targeted Approach to Implementing Ca Isotopes to Trace Fluid Sources in Rodingites Using the Major Element Content of Mineral Separates"

Booth #B-47

This study investigates rodingites from the Dun Mountain Ophiolite, New Zealand. Rodingites form when mafic dikes are altered by Ca-rich fluids originating from either clinopyroxene breakdown during serpentinization or sediment-derived subduction fluids. We hypothesize that serpentinite-derived fluids form rodingites with Ca isotope ratios (δ44/40Ca) similar to bulk silicate Earth (BSE; δ 44/40Ca ≈ 0.95‰; Kang et al., 2017), whereas sediment-derived fluids will result in deviations from this value. Initial garnet and clinopyroxene δ 44/40Ca data deviate from BSE (−0.29 to +1.07‰; avg. = +0.42‰), suggesting formation by sediment-derived subduction fluids. However, inconsistent δ 44/40Ca values within the same outcrop (CH23-1B = −0.1‰; CH23-1E = +0.57‰) and anomalously large values (CH23-2E = −1.38‰; CH23-3 = +2.61‰) introduce ambiguity to our interpretations. To gain additional insights into the rodingites and aid in selecting samples for subsequent δ 44/40Ca analyses, we selected single-phase separates (diopside, grossular, hibschite, and vesuvianite) and measured their major element compositions using electron probe microanalysis. We found that Cr_2O_3 and TiO_2 contents vary with mineral subclassification (grossular Cr_2O_3 = 0-0.2 wt.%; hibschite Cr_2O_3 = 0-0.8 wt.%), mineral formation mechanism (magmatic/relict diopside TiO_2 = 0-0.5 wt.%; hydrothermal diopside 0-0.15 wt.%) and serpentinite host characteristics (vesuvianite in subduction-altered serpentinites TiO_2 = 0-3.0 wt.%; vesuvianite in unaltered serpentinites TiO_2 = 0-0.6 wt.%). Although the source of TiO_2 variability is unclear, separates enriched in Cr_2O_3 suggest formation

by serpentinite-derived fluids. Mineral separates with endmember Cr_2O_3 and TiO_2 contents may be ideal targets for Ca isotope analyses aimed at constraining fluid sources involved in rodingitization.

Sedimentology & Stratigraphy (2 Participants)

Rivera, Paola Salas., Brunner, Benjamin., Igomu, Charles

"Megaquartz and detrital mica pin down the origin of lacustrine dolostone and gypsum associated with the Moab, Utah salt wall"

Booth #B-32

At the Moab Valley salt wall, laminated dolostones interfinger with fluvial siliciclastic sediments of the Triassic Chinle Formation and are stacked atop gypsic caprock of the Pennsylvanian Paradox Formation. The stratigraphic relationship, along with sediment petrography, suggests a Triassic lacustrine origin for primary dolostones at the diapir margin. Dissolution of samples yielded megaquartz and detrital mica grains from laminated, disturbed, and brecciated dolostone samples, as well as from some, but not all, gypsum samples collected near the dolostones. Megaquartz with boxwork fabric, interpreted as dolomite casts, is characteristic of sabkha environments.

We propose that a hypersaline lake formed at the exposed Moab Valley salt wall under arid conditions, as indicated by the absence of macroscopic fossils and pollen and consistent with regional aridification trends in the Late Triassic. Whereas limestone was deposited in correlative lakes, i.e., the Owl Rock Member of the Chinle Formation, dolomite formation at the Moab Valley site was driven by elevated Mg:Ca ratios due to co-precipitation with gypsum. Detrital mica found in both dolostone and gypsum, indicates some gypsum at the site may be Triassic, rather than exclusively Pennsylvanian in age. Dissolution of Mg-bearing minerals (e.g., Mg–K chlorides and sulfates), in the salt wall could have contributed to elevated Mg:Ca ratios and thus the local carbonate chemistry, differentiating it from other contemporaneous lacustrine systems. Our model for primary dolostone formation in lacustrine settings at the Moab Valley salt wall may be applicable to other locations where dolostones are found proximal to diapir margins.

Kohn, Jennifer., Sylvester, Zoltán., Covault, Jacob A

"Distinct Depositional Processes for Permian Basin Laminated Siltstones Inferred from Quantitative Grain-Scale Petrography"

Booth #B-33

Laminated siltstones are the most abundant facies within Leonardian and Guadalupian strata in the Permian Basin, yet their depositional mechanism remains debated. Proposed processes include suspension settling from aeolian dust storms, emplacement of distal turbidity currents, and settling from hypopycnal flows. This facies is characterized by striking, varve-like alternations of light-colored, millimeter-thick silty layers and thinner, organic-rich dark layers, and form extensive sheets that drape the basin floor. Individual laminations can exhibit lateral continuity spanning several kilometers, indicating a regional scale depositional process. We analyzed core and thin sections from representative laminated siltstone deposits in the Spraberry and Cherry Canyon formations of the Midland and Delaware basins, respectively, and apply an automated point-count workflow (Sylvester et al., 2025) to acquire large datasets (n > 10,000) for petrographic analysis to evaluate their depositional processes.

Samples from laminated facies are divided into “coarse”, “mixed” and “muddy” sub-facies. Turbidite facies with classic Bouma expression are also common and are visually distinct from laminated facies in core. Grain orientations show subtle differences among broad facies, with turbidite samples displaying weak indications of preferred grain alignment and laminated samples lacking this orientation signal. Kernel density estimates (KDEs) of grain size distributions reveal more systematic differences between laminated sub-facies. Within the Spraberry Formation, the coarse laminated siltstone exhibits a peak grain-size of ~52 microns, which is larger than for mixed and muddy laminated sub-facies. Samples from the Cherry Canyon Formation show similar grain-size differences between sub-facies; however, Cherry Canyon grain sizes are coarser on average.

Grain-size distributions of the laminated siltstone facies overlap with those of modern aeolian dust storm deposits over the Arabian Gulf, supporting a wind-blown origin for these facies. Additionally, patterns of grain-size fining away from coastal erg sources along the modern Arabian Gulf might explain for fining trends from coarser laminated siltstones toward mixed and muddy end members. These results support the interpretation that laminated siltstones represent depositional processes distinct from turbidity currents and are consistent with widespread suspension settling, potentially driven by large-scale aeolian dust events.

Economic Geology & Critical Minerals (3 Participants)

O’Bryan, Holiday

“Relevant or Redundant: Evaluating the Disbandment of the U.S. Bureau of Mines”

Booth #B-34

Critical minerals have increasingly become central to discourse concerning national security in the United States, reflecting concerns over economic resilience,

energy and resource dependence, and military preparedness. While contemporary debates often focus on international tensions, the roots of America's current mineral vulnerability can be traced to a number of national bureaucratic decisions, primarily the disbandment of the US Bureau of Mines in 1996. This work evaluates the 1996 disbandment through a thematic analysis of key documents from Congress and the public at large. We find that core debates concerning the survival of the Bureau centered on its perceived relevance or redundance and that the final decision was based largely on budgetary considerations. The 1996 disbandment was also heavily influenced by political battles beyond the Bureau including the creation of the National Performance Review and the Republican Contract with America. This analysis is employed to assess the state of modern American critical minerals policy and considers whether the reestablishment of a central federal body concerned with critical minerals is necessary or warranted in today's geopolitical environment. This work finds that the absence of a federal institution dedicated to mining research and policy weakened domestic mineral capacity and that the consequences of the disbandment of the Bureau significantly impacted American minerals policy.

Clark, Shelby; Locmelis, Marek

"Understanding lower crustal sulfide ore systems: Insights from ultramafic pipes in the Ivrea-Verbano Zone, Italy"

Booth #B-35

The decline in discoveries of economically significant magmatic sulfide deposits in the uppermost crust requires extending the search space to deeper (exhumed) levels to meet future metal demands. One area that allows to study the genesis of deep lithospheric sulfide systems is the Ivrea-Verbano Zone (IVZ) in Italy, an exhumed cross section of lower continental crust and sub-continental lithospheric mantle. The IVZ hosts a strongly metasomatized and sulfide-mineralized ultramafic pipe system wherein sulfides are intergrown, or otherwise associated with, carbonates and hydrous silicates. We expand previous research of the 249 Ma Valmaggia pipe (intruded in Lower Permian gabbroic units) to the less-studied 277 Ma Fei di Doccio pipe (intruded at a higher level into Paleozoic amphibolite facies metapelites). We find that, similarly to Valmaggia, the Fei di Doccio pipe contains genetically associated sulfides, carbonates, and hydrous silicates with overall similar elemental patterns. Our results emphasize that the pipes are genetically linked and that sulfur- and carbon-rich mantle fluids played a critical role in mobilizing metals in the deep lithosphere and fertilizing the lower crust in metals. Future research will focus on understanding the fluid path architecture in the IVZ to help develop exploration models for Ni-Cu-PGE in exhumed lower crust.

Swain, Regan; Locmelis, Marek; Clark, Shelby

“The Genesis of the Bourbon Iron Ore Deposit in the Geodynamic Context of the St. Francois Mountains Terrane in Southeast Missouri, USA”

Booth #B-36

Three main types of iron ore deposits exist in the Mesoproterozoic Eastern Granite-Rhyolite province outcropped in southeast Missouri, USA, i.e., Iron Oxide Apatite (IOA), Iron Oxide Copper-Gold (IOCG), and low temperature hydrothermal iron ore deposits. Although there are no current iron ore mining activities in Missouri, there is renewed interest in these historic deposits because of their potential to contain economically significant amounts of ‘critical minerals’, especially Ni, Co, and rare earth elements. Most iron ore deposits in Missouri are thought to have been emplaced at the same time ~1.44 Ga ago and thus are hypothesized to be genetically related. However, little is known about the magmatic-hydrothermal plumbing system that might have formed them. Understanding this plumbing system will help to identify areas that are most likely to contain undiscovered, critical mineral-rich, iron ore deposits. To develop such a ‘Mineral Systems Concept’ for iron ore exploration in Missouri, it is pivotal to understand how individual deposits in the region formed and what possibly connects them. For this purpose, this project investigates the subsurface Bourbon iron ore deposit. The deposit was identified as a potential prospect in the 1930s through magnetic and gravity remote sensing surveys along with a handful of other smaller potential prospects in the area. Although the Bourbon deposit has been drilled for exploration in the past, it has not been mined and its genesis remains to be fully understood. Drill core samples show that the Bourbon deposit consists of a 100 to 200-m-thick massive magnetite ore body with minor secondary hematite underneath ~600 m of rhyolitic overburden. A comparison of bulk rock data for Bourbon magnetite ore to magnetite ore from the nearby Kratz Spring (IOA) and Shephard Mountain (low temperature hydrothermal) deposits shows that the bulk rock chemistry of the Bourbon mineralization is notably similar to the magmatic hydrothermal IOA mineralization at Kratz Spring. An IOA origin for Bourbon is also consistent with its deep emplacement level and presence of brecciated intervals. Future work will investigate possible genetic links between the Bourbon deposit and other IOA systems in the region and interpret the findings within the framework of the geodynamic evolution of the St. Francois Mountain terrane to guide mineral exploration.